THYROID
Volume 28, Number 11, 2018

DOI: 10.1089/thy.2017.0561

High Thyrotropin Is Associated with Reduced Hippocampal Volume in a Population-Based Study from Germany

Till Ittermann,[1] Katharina Wittfeld,[2,3] Matthias Nauck,[4,5] Robin Bülow,[6] Norbert Hosten,[6] Henry Völzke,[1] and Hans J. Grabe[2,3]

Background: Previous patient studies suggest that thyroid dysfunction affects volumes of particular regions of the brain. So far, population-based data related to this topic are lacking. The aim of this study was to investigate associations of serum levels of thyrotropin (TSH), free triiodothyronine, and free thyroxine (fT4) with total brain volume, gray matter volume, white matter volume (WMV), and hippocampal volume (HV) in a population-based study.

Methods: Data on 2557 individuals were pooled from two independent population-based surveys of the Study of Health in Pomerania conducted in Northeast Germany. Brain volumes were determined from images derived from 1.5 T magnetic resonance imaging. Low and high TSH were defined using the cutoffs 0.40 and 3.29 mIU/L, respectively. Associations between thyroid hormone levels and segmented brain volumes were analyzed by linear regression models. Further, voxel-based morphometry was conducted to search for associations with thyroid hormone levels in a hypothesis-free way throughout the whole brain. All models were adjusted for confounders.

Results: Only 9/70 individuals with high TSH had low free triiodothyronine or fT4 levels. Individuals with high TSH had significantly lower total brain volume ($\beta = -26.9$ [confidence interval (CI) −49.0 to −4.8]; $p = 0.017$), WMV ($\beta = -16.1$ [CI −29.4 to −2.7]; $p = 0.018$), and HV ($\beta = -223$ [CI −395 to −50]; $p = 0.011$) than individuals with TSH within the reference range, while low TSH was not significantly associated with any of the brain volumes. Voxel-based morphometry analyses revealed a significant positive association with serum fT4 levels in the left middle frontal gyrus.

Conclusions: In conclusion, the results of this study indicate that the subclinical hypothyroid state may lead to a reduced brain volume affecting particularly HV in younger subjects and WMV, which might correspond to subtle microstructural changes in white matter fiber tracts or myelination of the axones. Gray matter seems not to be affected by subclinical hypothyroid states.

Keywords: thyrotropin, hypothyroidism, brain volume, gray matter, hippocampus, population-based

Introduction

It is well established that maternal thyroid hormones play a prominent role in fetal brain development (1). In line with this, in 646 mother–child pairs, data from the Generation R study demonstrated a significant lower gray matter volume (GMV) in children from mothers with high or low serum free thyroxine levels (fT4) compared to children delivered from mothers with fT4 levels within the reference range (2). This indicates that thyroid hormones obviously have an extreme impact on brain development. Likewise, in adults, it has been previously reported that thyroid dysfunction is associated with functional disturbances of the brain such as cognitive impairment (3), neurodegenerative disorders (4), dementia (5), depression (6), and anxiety (6). Similarly, there is also evidence that thyroid dysfunction affects brain morphology. Results from the Rotterdam Study showed that high fT4 levels are associated with larger total brain volume (TBV) and white matter volume (WMV) in young people, while older people with high fT4 levels had smaller TBV and WMV (7). Furthermore, results from three smaller studies suggest that thyroid function affects specific regions of the brain (8–10). Using the voxel-based morphometry (VBM) technique, one study demonstrated a lower GMV in

[1]Institute for Community Medicine, [2]Institute for Psychiatry and Psychotherapy, and [3]German Center for Neurodegenerative Diseases (DZNE), Site Rostock/Greifswald, Greifswald, Germany.
[4]Institute for Clinical Chemistry and Laboratory Medicine; [5]DZHK (German Centre for Cardiovascular Research), Partner Site Greifswald; [6]Institute of Diagnostic Radiology and Neuroradiology, University Medicine Greifswald, Greifswald, Germany.

specific brain regions related to memory, emotion, vision, and motor planning of 51 hyperthyroid patients in comparison to controls (10). Another study induced hyperthyroidism in 29 healthy subjects and showed an increase in GMV in the right posterior cerebellum and a decrease in GMV in the bilateral visual cortex and anterior cerebellum (8). One further study demonstrated significantly reduced WMV and GMV in 10 hypothyroid patients compared to 10 matched controls in VBM analyses (9). Likewise, small patient studies demonstrated a significant lower hippocampal volume (HV) in congenital (11) or adult-onset hypothyroidism (12).

So far, the association between thyroid dysfunction and brain volumes has only been investigated in small patient studies, and it is debatable whether these findings can be extended to the general population. Against this background, this study aimed to investigate whether high thyrotropin (TSH) levels are associated with lower GMV, WMV, and HV in data derived from two population-based studies conducted in northeast Germany. Brain volume parameters were derived from brain magnetic resonance imaging (MRI). In the analyses, two approaches were followed. The first approach looked at whether thyroid hormone levels were associated with total GMV, WMV, and HV, while in the second approach, VBM analyses were performed to investigate potential associations of thyroid biomarkers with local GMV in a hypothesis-free approach.

Methods

General population sample

Data from the population-based Study of Health in Pomerania (SHIP) were analyzed (13–15). The target population of the first cohort was comprised of adult German residents in northeast Germany living in three cities and 29 communities with a total population of 212,157. A two-stage stratified cluster sample of adults with German citizenship aged 20–79 years (baseline) was randomly drawn from local registries. The net sample (without migrated or deceased persons) comprised 6267 eligible subjects, of whom 4308 Caucasian subjects participated at baseline SHIP-0 between 1997 and 2001. The follow-up examination (SHIP-1) was conducted five years after baseline and included 3300 subjects. From 2008 to 2012, the third phase of data collection (SHIP-2; $N=2333$) was carried out. In this study, an association of diagnosed hypothyroidism with depression and anxiety was previously demonstrated (6). Concurrent with SHIP-2, a second sample called SHIP-Trend-0 ($N=4420$) was drawn from the same area in 2008, and similar examinations were undertaken.

Subjects from SHIP-2 and SHIP-Trend-0 were asked to participate in a whole-body MRI assessment (16,17). After exclusion of subjects who refused participation or who fulfilled exclusion criteria for MRI (e.g., cardiac pacemaker), 1163 subjects from SHIP-2 and 2154 subjects from SHIP-Trend-0 underwent MRI scanning ($N=3317$; Fig. 1). SHIP and SHIP-Trend were approved by the local ethics committee. Informed written consent was obtained from all participants.

Complete data sets, including thyroid levels, education, body mass index (BMI), alcohol consumption, smoking habits, and marital status, were available from 2884 subjects. After exclusion of medical conditions (e.g., a history of cerebral tumor, stroke, Parkinson disease, multiple sclerosis, epilepsy, hydrocephalus, enlarged ventricles, or pathological lesions) or technical reasons (e.g., severe movement artifacts or inhomogeneity of the magnetic field), 2595 subjects were available (Fig. 1). Based on the homogeneity check of the CAT12 toolbox (developed by Christian Gaser, University of Jena, Germany; www.neuro.uni-jena.de/), 38 extreme outliers were excluded, resulting in a final sample of 2557 individuals for analyzing TBV. Further, for the VBM analyses, all subjects >65 years of age were excluded in order to minimize the influence of neurodegenerative effects, resulting in a final sample of 2084 individuals in this analysis. For sensitivity analyses, additional VBM analyses were conducted on a subset of 1893 subjects by excluding those taking thyroid medication.

Assessments

All images were obtained using a 1.5 T Siemens MRI scanner (Magnetom Avanto; Siemens Medical Systems,

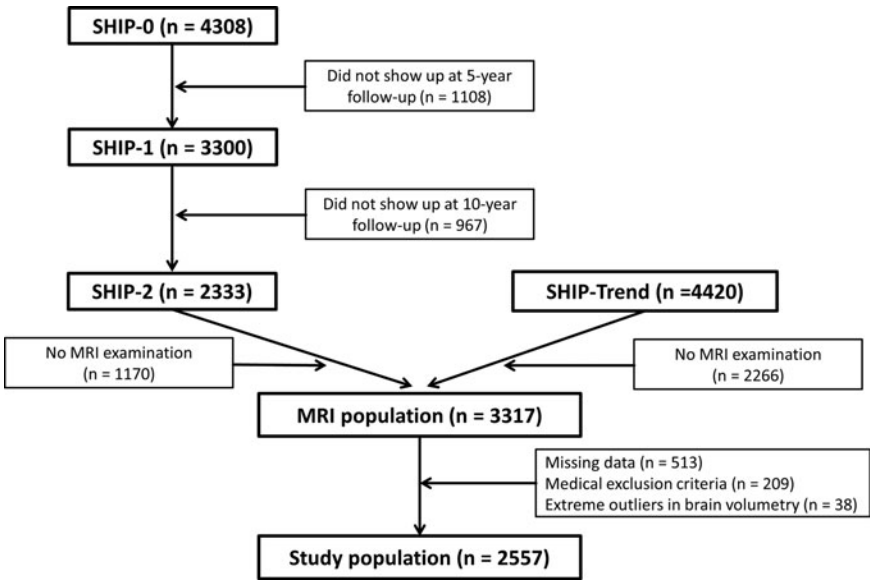

FIG. 1. Consort diagram.

Erlangen, Germany) with a T1-weighted magnetization prepared rapid acquisition gradient echo (MPRAGE) sequence and the following parameters: axial plane, TR = 1900 ms, TE = 3.4 ms, and flip angle = 15°, with an original resolution of 1.0 mm × 1.0 mm × 1.0 mm. The HV, GMV, and WMV were determined within the recon-all pipeline of FreeSurfer 5.1. Mean HV was defined as the mean volume of the left and the right hemisphere. TBV was defined as the sum of GMV and WMV.

For the VBM, the images were preprocessed with SPM12 (Wellcome Trust Centre for Neuroimaging, University College London, London, United Kingdom) and the CAT12 toolbox (developed by Christian Gaser, University of Jena, Germany; www.neuro.uni-jena.de/). The images were bias corrected, spatially normalized using the high-dimensional DARTEL normalization, segmented into the different tissue classes, modulated for affine transformations and nonlinear warping, and smoothed by a Gaussian kernel of 8 mm full width at half maximum. Homogeneity of GM images was checked using the covariance structure of each image with all other images, as implemented in the check data quality function of the CAT12 toolbox.

Non-fasting blood samples were taken between 7:00am and 4:00pm. Serum TSH, free triiodothyronine (fT3), and fT4 concentrations were analyzed in the central laboratory of the University Medicine Greifswald by a homogeneous, sequential, chemiluminescent immunoassay based on LOCI® technology (Dimension Vista® System Flex® reagent cartridge; Siemens Healthcare Diagnostics Inc., Newark, DE). The analytical measuring range was 0.005–100 mIU/mL, 0.1–8.0 ng/dL, and 0.50–30.00 pg/mL for TSH, fT4, and fT3, respectively. Low and high serum TSH concentrations were defined using the cutoffs 0.49 and 3.29 mIU/L, respectively, which were recently established for the study region (18).

Smoking status, alcohol consumption, and educational status were assessed by computer-assisted personal interviews. Smokers were categorized into three categories: lifetime nonsmokers, former smokers, and current smokers. Alcohol consumption was evaluated as beverage-specific alcohol consumption (beer, wine, and distilled spirits) on the last month preceding the examination, and the mean daily alcohol consumption was calculated using beverage-specific pure ethanol volume proportions (19). Education was categorized according to the German three-level school system: low, <10 years; intermediate, 10 years; and high, >10 years. Height and weight were measured for the calculation of the BMI, being weight (kg)/height^2 (m^2).

Statistical methods

All results are reported as pooled data of SHIP-Trend-0 and SHIP-2. Stratified by thyroid function status, continuous data are expressed as median and 25th and 75th percentile, and categorical data as absolute numbers and percentages. The association between thyroid hormone tests and brain volumes were analyzed by linear regression models adjusted for age, sex, BMI, alcohol consumption, smoking status, education, and time of blood sampling. Continuous exposure variables (TSH, fT3, fT4) were power transformed to reduce the effect of outliers on the results (20). Multivariable fractional polynomials were tested to account for potential nonlinear associations of exposure or confounders with the outcome. Interactions of thyroid hormones with age and sex were tested for all outcomes. Inverse probability weights

Table 1. Characteristics of the Study Population Stratified by TSH Status

	0.40 mIU/L ≤ TSH <3.29 mIU/L (n = *2285*)	*TSH <0.40 mIU/L* (n = *229*)	*TSH ≥3.29 mIU/L* (n = *70*)
Age, years	51 (41; 61)	57 (47; 67)	49 (37; 62)
Males	1041 (46.1%)	100 (43.7%)	25 (35.7%)
Body mass index, kg/m^2	26.9 (24.3; 30.2)	27.3 (24.4; 30.6)	25.7 (22.6; 29.1)
Smoking status			
Former	811 (35.9%)	97 (42.4%)	30 (42.8%)
Current	523 (23.2%)	55 (24.0%)	17 (24.3%)
Alcohol consumption, g/day	4.4 (1.3; 11.7)	2.8 (0.5; 7.4)	3.9 (0.7; 9.1)
Education			
Low	328 (14.5%)	55 (24.0%)	10 (14.3%)
Medium	1284 (56.9%)	116 (50.7%)	38 (54.3%)
High	646 (28.6%)	58 (25.3%)	22 (31.4%)
General health			
Good or very good	1992 (88.4%)	187 (82.4%)	58 (84.1%)
Less good or bad	262 (11.6%)	40 (17.6%)	11 (15.9%)
Total brain volume, mL	1147 (1068; 1236)	1127 (1047; 1207)	1096 (1021; 1189)
Gray matter volume, mL	641 (599; 690)	625 (578; 669)	630 (580; 679)
White matter volume, mL	504 (462; 549)	496 (461; 542)	473 (447; 520)
Right hippocampal volume, mm^3	3997 (3707; 4291)	3890 (3568; 4168)	3775 (3549; 4136)
Left hippocampal volume, mm^3	3907 (3618; 4204)	3769 (3470; 4071)	3619 (3485; 4056)
TSH, mIU/L	1.19 (0.86; 1.60)	0.35 (0.26; 0.44)	3.90 (3.61; 5.17)
fT3, pmol/L	4.65 (4.30; 5.06)	4.76 (4.35; 5.12)	4.44 (4.08; 4.89)
fT4, pmol/L	13.3 (12.3; 14.4)	14.4 (13.2; 15.5)	12.7 (11.3; 14.0)
Thyroid medication	208 (9.2%)	56 (24.5%)	16 (22.9%)

Continuous data are expressed as median and 25th and 75th percentile; categorical data are expressed as absolute numbers and percentages.

TSH, thyrotropin; fT3, free triiodothyronine; fT4, free thyroxine.

were applied to consider dropouts of individuals between SHIP-0 and SHIP-2 and between the basic and the MRI examinations. The intention behind these weights is to weight up the impact of individuals from groups who are more likely to drop out of the study and to weight down the impact of individuals from groups who are less likely to drop out in the regression analyses. To calculate these weights, logistic regression models were used, with participation at the MRI examination as outcome and sociodemographic, behavioral, and cardiovascular risk factors from the core examinations as explanatory variables. Additionally, for SHIP-2 participants, weights were computed for the dropout from SHIP-0 to SHIP-2, and these weights were multiplicatively combined with the MRI weights. This approach aimed to improve the representativeness of the analyses. A p-value of <0.05 was considered as statistically significant. All analyses were performed with Stata v14.1 (Stata Corp., College Station, TX).

For VBM analysis, SPM12 was used to analyze the preprocessed GM segments in three separate regression analyses between GM volume and the power-transformed levels of TSH, fT3, and fT4 adjusted for age, sex, education, BMI, alcohol consumption, smoking habits, marital status, and intracranial volume as covariates in all models. In a VBM analysis, a single statistical test is carried in each voxel of the brain. To take into account multiple testing, family-wise error (FWE) corrected peak-level p-values with a threshold of 0.05 to reach significance were used.

Results

Of the 2557 individuals in the study population, there were 229 with low TSH (47 with high fT3 or fT4) and 70 with high TSH (9 with low fT3 or fT4). There were only two individuals with TSH levels >10 mIU/L. Individuals with low TSH were in median older, more often former smokers, less educated, and reported more often a less good or bad general health than individuals with serum TSH levels within the reference range (Table 1). Median brain volumes differed only slightly between individuals with low TSH and individuals with TSH within the reference range. Individuals with high TSH were more often females, had a lower BMI, smoked more often, and reported more often a less good or bad general health than individuals with serum TSH levels within the reference range. Median brain volumes were lower in individuals with high TSH than in individuals with TSH within the reference range.

In multivariable linear regression models adjusted for confounders, serum TSH levels were inversely associated with TBV, WMV, and left HV (Table 2 and Fig. 2). Individuals with high TSH had significantly lower TBV, WMV as well as mean, right, and left HV than individuals with normal TSH. Individuals with low TSH had a significantly lower left HV than individuals with serum TSH levels within the reference range. No further significant associations were observed of low TSH with any of the brain volumes. Likewise, neither serum fT3 nor serum fT4 levels were significantly associated with TBV, GMV, WMV, or HV. All the observed significant association were confirmed after excluding individuals with high TSH but low fT3 or fT4 and individuals with low TSH but high fT3 or fT4.

For the outcomes TBV, GMV, and WMV, no significant interactions of TSH were detected with age (TBV, $p = 0.664$;

Table 2. Association of Thyroid Hormone Levels with Brain Volumes

	Brain volumes, β [confidence interval]					
	Total	*Gray matter*	*White matter*	*Mean HC*	*Right HC*	*Left HC*
TSH, mIU/L	−34.8 [−61.6 to −8.0]*	−13.0 [−26.4 to 0.5]	−20.5 [−36.4 to −4.7]*	−175 [−382 to 33]	−86 [−194 to 22]	−128 [−232 to −24]*
TSH <0.40 mIU/L[a]	−6.9 [−19.7 to 6.0]	−4.8 [−11.8 to 2.1]	−1.5 [−8.7 to 5.7]	−94 [−196 to 9]	−37 [−92 to 17]	−54 [−105 to −3]*
TSH ≥3.29 mIU/L[a]	−26.9 [−49.0 to −4.8]*	−9.3 [−20.3 to 1.6]	−16.1 [−29.4 to −2.7]*	−223 [−395 to −50]*	−107 [−196 to −17]*	−126 [−217 to −36]*
fT3, pmol/L	−3.8 [−33.4 to 25.9]	3.1 [−12.7 to 18.9]	−6.3 [−23.5 to 10.8]	−24 [−249 to 201]	3 [−116 to 122]	−16 [−131 to 98]
fT4, pmol/L	−0.1 [−29.6 to 29.3]	0.3 [−15.3 to 15.9]	−2.1 [−14.9 to 19.0]	−66 [−281 to 148]	−30 [−143 to 84]	−27 [−136 to 82]

Data are expressed as β coefficients and confidence intervals derived from a linear regression adjusted for age, sex, body mass index, smoking status, alcohol consumption, education, and time of blood sampling. Continuous values of TSH, fT3, and fT4 were power transformed to minimize the effect of outliers. Mean hippocampal (HC) volume was calculated as the sum of right and left hippocampal volume.

[a]In comparison to TSH within the reference range.

*$p < 0.05$.

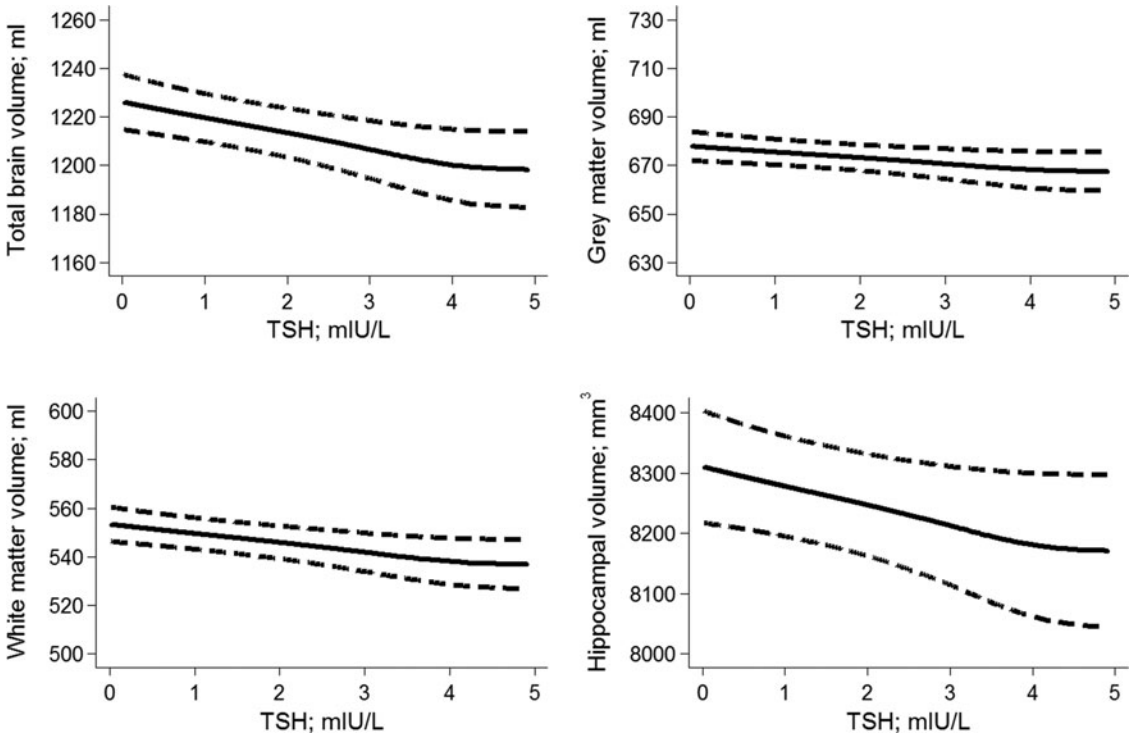

FIG. 2. Association between serum thyrotropin (TSH) levels and brain volumes adjusted for confounders.

GMV, $p = 0.757$; WMV, $p = 0.653$) or sex (TBV, $p = 0.965$; GMV, $p = 0.603$; WMV, $p = 0.716$), but there was a significant interaction of TSH with age ($p = 0.055$) but not with sex ($p = 0.440$) for mean HV. TSH was significantly associated with mean HV for individuals <50 years of age but not for individuals ≥50 years of age (Fig. 3). For right and left HV, similar effects were observed than for mean HV (right HV, $p = 0.066$; left HV, $p = 0.064$). For all outcomes, no significant interaction was observed of TSH with current smoking (TBV, $p = 0.639$; GMV, $p = 0.246$; WMV, $p = 0.748$; HV, $p = 0.120$) or thyroid medication (TBV, $p = 0.509$; GMV, $p = 0.360$; WMV, $p = 0.724$; HV, $p = 0.777$).

In the VBM analyses, a cluster of five voxels was detected in the left middle frontal gyrus that is significantly positive associated with serum fT4 ($p = 0.026$; MNI [–42, 24, 42]). The corresponding VBM without the subjects with a thyroid medication showed an even stronger effect in this region ($p = 0.007$; MNI [–42, 24, 42], 29 voxels). No further significant associations of TSH or fT3 were found in the VBM analyses. Since the significant cluster is part of the Brodmann area 9 (BA9), the GM volume of BA9 was extracted from the CAT12 GM segmentations of the MRI scans. The BA9 volume correlated significantly with the HV ($R^2 = 0.39$). A significant inverse association of serum TSH levels was

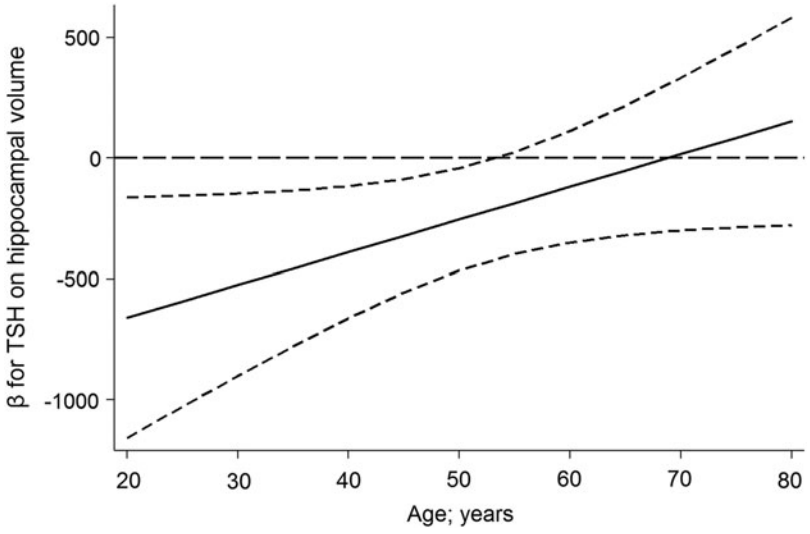

FIG. 3. Association between serum TSH levels and hippocampal volume for different ages.

found with overall BA9 volume ($p = 0.032$), whereas serum fT3 ($p = 0.888$) or fT4 ($p = 0.637$) levels were not significantly associated with overall BA9 volume.

Discussion

In a population-based cross-sectional sample, inverse associations of serum TSH levels with TBV, WMV and HV, but not with GMV, are demonstrated. Particularly, high TSH levels were associated with a decrease in brain volumes. In contrast, no significant associations of fT3 or fT4 levels were detected with any of the brain volumes. While no significant association of thyroid hormone levels was observed with overall GMV, VBM analyses revealed a positive association of fT4 with a region in the left middle frontal gyrus, which is located in BA9.

These findings are in partial agreement with a patient study in 11 hypothyroid adults and nine age-matched controls, in which right but not left HV was significantly decreased in hypothyroidism (12). The lack of a significant association for left HV in the adult study may be explained by low statistical power (12). In another study, congenital hypothyroidism was significantly associated with right and left HV in children and adolescents (11). In a further study, HV was significantly lower in 24 children aged 9–12 years delivered from mothers with hypothyroidism during pregnancy than in 30 controls delivered from mothers without hypothyroidism during pregnancy (21). In the present study, high TSH was inversely associated with both right and left HV, but the study failed to demonstrate significant associations of serum fT3 or fT4 levels with HV. This might be related to the fact that out of the 70 individuals with high TSH, only nine had low fT3 or fT4 levels. After excluding these nine individuals, the association between high TSH and HV remained statistically significant, suggesting that not only overt but also subclinical hypothyroidism is associated with a reduced HV.

There are several potential mechanisms explaining an association of hypothyroidism with a reduced HV. First, the hippocampus may be an important target region for thyroid hormones because the density of thyroid hormone receptors in the hippocampus is high (22,23). Thus, a lack of thyroid hormones may lead to an inadequate supply of the hippocampus with T3 or T4. Second, animal experiments suggest that adult-onset hypothyroidism affects the pyramidal cells of the hippocampus (24–26). These studies demonstrated that in hypothyroidism the volume of the pyramidal cell layer in the hippocampal CA3 region is decreased because of an altered neuronal packing (24–26). Likewise, it has been reported that hypothyroidism reduces the total number of pyramidal cells in the hippocampal CA1 region (24). Furthermore, it has been proposed that hypothyroidism at a younger age may permanently change hippocampal function and in consequence HV (27), which fits well with the present finding of a significant inverse association between TSH and HV mainly for those aged <50 years.

In this study, inverse associations were observed of serum TSH levels not only with HV but also with BA9 volume, suggesting that hypothyroidism may result in cognitive impairment. BA9 is involved in short-term memory (28) and correlates with the hippocampus. In agreement with these findings, two smaller studies conducted in 81 (29) and 337 (30) elderly individuals demonstrated associations of subclinical hypothyroidism with cognitive impairment. The majority of studies, however, failed to substantiate significant associations of subclinical hypothyroidism (31–33) or serum TSH levels (34,35) with cognitive impairment in population-based data from individuals aged ≥65 years. Results from the Rotterdam Study demonstrated that higher TSH is associated with a lower dementia risk in both the full and the normal range of thyroid function (5). In line with this, that study reported a positive association between serum TSH levels and better global cognitive scores. However, thyroid function was not related to subclinical vascular brain disease derived from MRI, which suggested nonvascular pathways leading to dementia.

In the present analyses, a significant inverse association was observed between high TSH and WMV but no association with overall or region-specific GMV. It might be important to acknowledge that the study largely investigated subjects with subclinical thyroid conditions only. The results do not point to large brain changes, and in fact, the effects on HV were only relevant in younger subjects (<50 years). It is unclear how the association with WMV can be explained. Although white matter hyperintensities were did not analyzed as a correlate of microvascular damage, the study by Chaker *et al.* found no sign of any association between thyroid function and vascular parameters in 9446 subjects (5). However, Singh *et al.* detected microstructural changes in the white matter fiber tracts of hypothyroid patients compared to controls in their diffusion tensor tractography study (36). These changes could in part explain the findings of reduced WMV in subclinical hypothyroidism.

In contrast to the current results, Chaker *et al.* found no significant association between serum TSH levels and TBV or GMV in data from 4683 individuals aged ≥45 years (7). However, they observed that individuals aged 45–70 years with low fT4 levels had lower TBV and WMV than individuals with normal fT4 levels, which somewhat indicates that the hypothyroid state may be associated with reduced brain volumes. In that study, serum fT4 levels were inversely associated with TBV and WMV in individuals >80 years of age (7), an association that points in the opposite direction than in younger individuals of that study. The authors explain their findings by better white matter integrity in younger than in older persons. In this study, no age-dependency of the associations was observed, which may be related to the fact that the study included only eight individuals >80 years.

The present findings are in partial agreement with a small patient study in which 10 untreated hypothyroid patients had significantly lower WMV in the cerebellum, right precentral gyrus, right inferior and middle frontal gyrus, right inferior occipital gyrus, and right inferior temporal gyrus, and significantly lower GMV in the cerebellum and left postcentral gyrus than 10 controls (9). In agreement with the current findings, a study with 25 hypothyroid patients with Hashimoto thyroiditis on levothyroxine treatment did not show any differences in GMV compared to 27 controls (37), indicating that levothyroxine treatment may protect against hypothyroidism-induced vulnerability of the brain. A study with 1047 participants aged >64 years showed that hypothyroidism was associated with lower performance in the mini mental status (38). In that study, half of the hypothyroid participants were unaware of their condition and not treated by thyroid medication. From those findings, it can be concluded

that elderly patients with impairment in cognition should be screened for hypothyroidism (38), but to decide on potential therapeutically consequences, randomized controlled trials are needed.

While inverse associations of serum TSH levels were observed with total HV, no significant clusters of the HV were detected in the whole brain VBM analyses of TSH. In the VBM analysis, all *p*-values are FWE-corrected because of multiple voxel-based comparisons. Thus, VBM-analyses have a lower statistical power than targeted single region volume analyses. Therefore, only large and regionally homogenous clusters or highly significant peak voxels can be discovered in VBM analyses.

To the best of the authors' knowledge, this is the first population-based study associating thyroid hormone levels with brain volumes. Strengths of this study are the large number of individuals investigated and the assessment of brain volumes with gold-standard methods. A limitation is the cross-sectional design of this study allowing no causative conclusions. Furthermore, the range of blood sampling time was eight hours, from 8:00am to 4:00pm. It has been described that thyroid hormones are prone to diurnal variations (39). Therefore, a sensitivity analysis was performed, adjusting additionally for time of blood sampling, which did not change the results significantly. Another limitation of the study is that the onset time of altered thyroid function is unknown. Likewise, no information was available on the intake of ''harder'' drugs such as heroin or cocaine, but it is believed that the number of individuals taking such drugs was very low in this study. To account for nonparticipation at the MRI examinations, inverse probability weighting was introduced, assuming a ''missing at random'' mechanism. This means that that the dropout is not completely at random but can be explained by available data. However, a potential selection bias due to a ''missing not at random'' mechanism cannot be totally ruled out, which means that the dropout is not completely explainable by existing data.

In conclusion, the results of this study indicate that the subclinical hypothyroid state may lead to a reduced brain volume affecting particularly HV in younger subjects and WMV, which might correspond to subtle microstructural changes in white matter fiber tracts or myelination of the axons. GM seems not to be affected by subclinical hypothyroid states. Longitudinal studies are needed to understand better the interaction with age-related parameters and the putative clinical impact of dysregulated thyroid function on brain-related disorders.

Acknowledgments

The Study of Health in Pomerania is part of the Community Medicine Research Network of the University Medicine Greifswald, which was funded by the German Federal Ministry for Education and Research, the Ministry for Education, Research and Cultural Affairs, and the Ministry for Social Affairs of the State Mecklenburg-West Pomerania. MRI scans in SHIP and SHIP-TREND have been supported by a joint grant from Siemens Healthineers, Erlangen, Germany, and the Federal State of Mecklenburg-West Pomerania. The project has received funding from the European Union's Horizon 2020 research and innovation program under grant agreement number 634453.

Author Disclosure Statement

H.J.G. has received speaker's honoraria and travel grants from Fresenius Medical care and Janssen. No other competing financial interests exist.

References

1. Korevaar TIM, Tiemeier H, Peeters RP 2018 Clinical associations of maternal thyroid function with fetal brain development:Epidemiological interpretation and overview of available evidence. Clin Endocrinol (Oxf) 2018 Apr 24 [Epub ahead of print]; DOI: 10.1111/cen.13724.
2. Korevaar TI, Muetzel R, Medici M, Chaker L, Jaddoe VW, de Rijke YB, Steegers EA, Visser TJ, White T, Tiemeier H, Peeters RP 2016 Association of maternal thyroid function during early pregnancy with offspring IQ and brain morphology in childhood: a population-based prospective cohort study. Lancet Diabetes Endocrinol **4:**35–43.
3. Rieben C, Segna D, da Costa BR, Collet TH, Chaker L, Aubert CE, Baumgartner C, Almeida OP, Hogervorst E, Trompet S, Masaki K, Mooijaart SP, Gussekloo J, Peeters RP, Bauer DC, Aujesky D, Rodondi N 2016 Subclinical thyroid dysfunction and the risk of cognitive decline: a meta-analysis of prospective cohort studies. J Clin Endocrinol Metab **101:**4945–4954.
4. Cappola AR, Arnold AM, Wulczyn K, Carlson M, Robbins J, Psaty BM 2015 Thyroid function in the euthyroid range and adverse outcomes in older adults. J Clin Endocrinol Metab **100:**1088–1096.
5. Chaker L, Wolters FJ, Bos D, Korevaar TI, Hofman A, van der Lugt A, Koudstaal PJ, Franco OH, Dehghan A, Vernooij MW, Peeters RP, Ikram MA 2016 Thyroid function and the risk of dementia: The Rotterdam Study. Neurology **87:**1688–1695.
6. Ittermann T, Volzke H, Baumeister SE, Appel K, Grabe HJ 2015 Diagnosed thyroid disorders are associated with depression and anxiety. Soc Psychiatry Psychiatr Epidemiol **50:**1417–1425.
7. Chaker L, Cremers LGM, Korevaar TIM, de Groot M, Dehghan A, Franco OH, Niessen WJ, Ikram MA, Peeters RP, Vernooij MW 2018 Age-dependent association of thyroid function with brain morphology and microstructural organization: evidence from brain imaging. Neurobiol Aging **61:**44–51.
8. Gobel A, Heldmann M, Gottlich M, Dirk AL, Brabant G, Munte TF 2015 Effect of experimental thyrotoxicosis on brain gray matter: a voxel-based morphometry study. Eur Thyroid J **4:**113–118.
9. Singh S, Modi S, Bagga D, Kaur P, Shankar LR, Khushu S 2013 Voxel-based morphometric analysis in hypothyroidism using diffeomorphic anatomic registration via an exponentiated lie algebra algorithm approach. J Neuroendocrinol **25:**229–234.
10. Zhang W, Song L, Yin X, Zhang J, Liu C, Wang J, Zhou D, Chen B, Lii H 2014 Grey matter abnormalities in untreated hyperthyroidism: a voxel-based morphometry study using the DARTEL approach. Eur J Radiol **83:**e43–48.
11. Wheeler SM, Willoughby KA, McAndrews MP, Rovet JF 2011 Hippocampal size and memory functioning in children and adolescents with congenital hypothyroidism. J Clin Endocrinol Metab **96:**E1427–1434.
12. Cooke GE, Mullally S, Correia N, O'Mara SM, Gibney J 2014 Hippocampal volume is decreased in adults with hypothyroidism. Thyroid **24:**433–440.

13. Volzke H, Alte D, Schmidt CO, Radke D, Lorbeer R, Friedrich N, Aumann N, Lau K, Piontek M, Born G, Havemann C, Ittermann T, Schipf S, Haring R, Baumeister SE, Wallaschofski H, Nauck M, Frick S, Arnold A, Junger M, Mayerle J, Kraft M, Lerch MM, Dorr M, Reffelmann T, Empen K, Felix SB, Obst A, Koch B, Glaser S, Ewert R, Fietze I, Penzel T, Doren M, Rathmann W, Haerting J, Hannemann M, Ropcke J, Schminke U, Jurgens C, Tost F, Rettig R, Kors JA, Ungerer S, Hegenscheid K, Kuhn JP, Kuhn J, Hosten N, Puls R, Henke J, Gloger O, Teumer A, Homuth G, Volker U, Schwahn C, Holtfreter B, Polzer I, Kohlmann T, Grabe HJ, Rosskopf D, Kroemer HK, Kocher T, Biffar R, John U, Hoffmann W 2011 Cohort profile: the study of health in Pomerania. Int J Epidemiol **40:**294–307.
14. Grabe HJ, Lange M, Wolff B, Volzke H, Lucht M, Freyberger HJ, John U, Cascorbi I 2005 Mental and physical distress is modulated by a polymorphism in the 5-HT transporter gene interacting with social stressors and chronic disease burden. Mol Psychiatry **10:**220–224.
15. John U, Greiner B, Hensel E, Ludemann J, Piek M, Sauer S, Adam C, Born G, Alte D, Greiser E, Haertel U, Hense HW, Haerting J, Willich S, Kessler C 2001 Study of Health In Pomerania (SHIP): a health examination survey in an east German region: objectives and design. Soz Praventivmed **46:**186–194.
16. Stein JL, Medland SE, Vasquez AA, Hibar DP, Senstad RE, Winkler AM, Toro R, Appel K, Bartecek R, Bergmann O, Bernard M, Brown AA, Cannon DM, Chakravarty MM, Christoforou A, Domin M, Grimm O, Hollinshead M, Holmes AJ, Homuth G, Hottenga JJ, Langan C, Lopez LM, Hansell NK, Hwang KS, Kim S, Laje G, Lee PH, Liu X, Loth E, Lourdusamy A, Mattingsdal M, Mohnke S, Maniega SM, Nho K, Nugent AC, O'Brien C, Papmeyer M, Putz B, Ramasamy A, Rasmussen J, Rijpkema M, Risacher SL, Roddey JC, Rose EJ, Ryten M, Shen L, Sprooten E, Strengman E, Teumer A, Trabzuni D, Turner J, van Eijk K, van Erp TG, van Tol MJ, Wittfeld K, Wolf C, Woudstra S, Aleman A, Alhusaini S, Almasy L, Binder EB, Brohawn DG, Cantor RM, Carless MA, Corvin A, Czisch M, Curran JE, Davies G, de Almeida MA, Delanty N, Depondt C, Duggirala R, Dyer TD, Erk S, Fagerness J, Fox PT, Freimer NB, Gill M, Goring HH, Hagler DJ, Hoehn D, Holsboer F, Hoogman M, Hosten N, Jahanshad N, Johnson MP, Kasperaviciute D, Kent JW Jr, Kochunov P, Lancaster JL, Lawrie SM, Liewald DC, Mandl R, Matarin M, Mattheisen M, Meisenzahl E, Melle I, Moses EK, Muhleisen TW, Nauck M, Nothen MM, Olvera RL, Pandolfo M, Pike GB, Puls R, Reinvang I, Renteria ME, Rietschel M, Roffman JL, Royle NA, Rujescu D, Savitz J, Schnack HG, Schnell K, Seiferth N, Smith C, Steen VM, Valdes Hernandez MC, Van den Heuvel M, van der Wee NJ, Van Haren NE, Veltman JA, Volzke H, Walker R, Westlye LT, Whelan CD, Agartz I, Boomsma DI, Cavalleri GL, Dale AM, Djurovic S, Drevets WC, Hagoort P, Hall J, Heinz A, Jack CR Jr, Foroud TM, Le Hellard S, Macciardi F, Montgomery GW, Poline JB, Porteous DJ, Sisodiya SM, Starr JM, Sussmann J, Toga AW, Veltman DJ, Walter H, Weiner MW, Bis JC, Ikram MA, Smith AV, Gudnason V, Tzourio C, Vernooij MW, Launer LJ, DeCarli C, Seshadri S, Andreassen OA, Apostolova LG, Bastin ME, Blangero J, Brunner HG, Buckner RL, Cichon S, Coppola G, de Zubicaray GI, Deary IJ, Donohoe G, de Geus EJ, Espeseth T, Fernandez G, Glahn DC, Grabe HJ, Hardy J, Hulshoff Pol HE, Jenkinson M, Kahn RS, McDonald C, McIntosh AM, McMahon FJ, McMahon KL, Meyer-Lindenberg A, Morris DW, Muller-Myhsok B, Nichols TE, Ophoff RA, Paus T, Pausova Z, Penninx BW, Potkin SG, Samann PG, Saykin AJ, Schumann G, Smoller JW, Wardlaw JM, Weale ME, Martin NG, Franke B, Wright MJ, Thompson PM 2012 Identification of common variants associated with human hippocampal and intracranial volumes. Nat Genet **44:** 552–561.
17. Hegenscheid K, Kuhn JP, Volzke H, Biffar R, Hosten N, Puls R 2009 Whole-body magnetic resonance imaging of healthy volunteers: pilot study results from the population-based SHIP study. Rofo **181:**748–759.
18. Ittermann T, Khattak RM, Nauck M, Cordova CM, Volzke H 2014 Shift of the TSH reference range with improved iodine supply in Northeast Germany. Eur J Endocrinol **172:** 261–267.
19. Alte D, Ludemann J, Piek M, Adam C, Rose HJ, John U 2003 Distribution and dose response of laboratory markers to alcohol consumption in a general population: results of the study of health in Pomerania (SHIP). J Stud Alcohol **64:** 75–82.
20. Royston P, Sauerbrei W 2008 Multivariable Model-Building: A Pragmatic Approach to Regression Analysis Based on Fractional Polynomials for Modelling Continuous Variables. John Wiley, Chichester, United Kingdom.
21. Willoughby KA, McAndrews MP, Rovet JF 2014 Effects of maternal hypothyroidism on offspring hippocampus and memory. Thyroid **24:**576–584.
22. de Jong FJ, den Heijer T, Visser TJ, de Rijke YB, Drexhage HA, Hofman A, Breteler MM 2006 Thyroid hormones, dementia, and atrophy of the medial temporal lobe. J Clin Endocrinol Metab **91:**2569–2573.
23. Lathe R 2001 Hormones and the hippocampus. J Endocrinol **169:**205–231.
24. Koromilas C, Liapi C, Schulpis KH, Kalafatakis K, Zarros A, Tsakiris S 2010 Structural and functional alterations in the hippocampus due to hypothyroidism. Metab Brain Dis **25:**339–354.
25. Madeira MD, Pereira A, Cadete-Leite A, Paula-Barbosa MM 1990 Estimates of volumes and pyramidal cell numbers in the prelimbic subarea of the prefrontal cortex in experimental hypothyroid rats. J Anat **171:**41–56.
26. Madeira MD, Sousa N, Lima-Andrade MT, Calheiros F, Cadete-Leite A, Paula-Barbosa MM 1992 Selective vulnerability of the hippocampal pyramidal neurons to hypothyroidism in male and female rats. J Comp Neurol **322:** 501–518.
27. Gilbert ME 2004 Alterations in synaptic transmission and plasticity in area CA1 of adult hippocampus following developmental hypothyroidism. Brain Res Dev Brain Res **148:**11–18.
28. Babiloni C, Ferretti A, Del Gratta C, Carducci F, Vecchio F, Romani GL, Rossini PM 2005 Human cortical responses during one-bit delayed-response tasks: an fMRI study. Brain Res Bull **65:**383–390.
29. Johnson LA, Hobson V, Jenkins M, Dentino A, Ragain RM, O'Bryant S 2011 The influence of thyroid function on cognition in a sample of ethnically diverse, rural-dwelling women: a project FRONTIER study. J Neuropsychiatry Clin Neurosci **23:**219–222.
30. Resta F, Triggiani V, Barile G, Benigno M, Suppressa P, Giagulli VA, Guastamacchia E, Sabba C 2012 Subclinical hypothyroidism and cognitive dysfunction in the elderly. Endocr Metab Immune Disord Drug Targets **12:**260–267.

31. de Jongh RT, Lips P, van Schoor NM, Rijs KJ, Deeg DJ, Comijs HC, Kramer MH, Vandenbroucke JP, Dekkers OM 2011 Endogenous subclinical thyroid disorders, physical and cognitive function, depression, and mortality in older individuals. Eur J Endocrinol **165:**545–554.
32. Formiga F, Ferrer A, Padros G, Contra A, Corbella X, Pujol R; Octabaix Study Group 2014 Thyroid status and functional and cognitive status at baseline and survival after 3 years of follow-up: the OCTABAIX study. Eur J Endocrinol **170:**69–75.
33. Parsaik AK, Singh B, Roberts RO, Pankratz S, Edwards KK, Geda YE, Gharib H, Boeve BF, Knopman DS, Petersen RC 2014 Hypothyroidism and risk of mild cognitive impairment in elderly persons: a population-based study. JAMA Neurol **71:**201–207.
34. Booth T, Deary IJ, Starr JM 2013 Thyroid stimulating hormone, free thyroxine and cognitive ability in old age: the Lothian Birth Cohort Study 1936. Psychoneuroendocrinology **38:**597–601.
35. Castellano CA, Laurin D, Langlois MF, Fortier M, Tessier D, Gaudreau P, Ferland G, Payette H, Lorrain D, Cunnane SC 2013 Thyroid function and cognition in the euthyroid elderly: a case-control study embedded in Quebec longitudinal study—NuAge. Psychoneuroendocrinology **38:** 1772–1776.
36. Singh S, Trivedi R, Singh K, Kumar P, Shankar LR, Khushu S 2014 Diffusion tensor tractography in hypothyroidism and its correlation with memory function. J Neuroendocrinol **26:**825–833.
37. Quinque EM, Karger S, Arelin K, Schroeter ML, Kratzsch J, Villringer A 2014 Structural and functional MRI study of the brain, cognition and mood in long-term adequately treated Hashimoto's thyroiditis. Psychoneuroendocrinology **42:**188–198.
38. Hogervorst E, Huppert F, Matthews FE, Brayne C 2008 Thyroid function and cognitive decline in the MRC Cognitive Function and Ageing Study. Psychoneuroendocrinology **33:**1013–1022.
39. Surks MI, Goswami G, Daniels GH 2005 The thyrotropin reference range should remain unchanged. J Clin Endocrinol Metab **90:**5489–5496.

Address correspondence to:
Till Ittermann, Dr. rer. med.
Institute for Community Medicine
Ernst Moritz Arndt University
Walther Rathenau Str. 48
D-17487 Greifswald
Germany

E-mail: till.ittermann@uni-greifswald.de

A MicroRNA Signature for Evaluation of Risk and Severity of Autoimmune Thyroid Diseases

Rebeca Martínez-Hernández,[1] Miguel Sampedro-Núñez,[1] Ana Serrano-Somavilla,[1] Ana M. Ramos-Leví,[1] Hortensia de la Fuente,[2,3] Juan Carlos Triviño,[4] Ancor Sanz-García,[5] Francisco Sánchez-Madrid,[2,3] and Mónica Marazuela[1]

[1]Department of Endocrinology, Hospital Universitario de la Princesa, Instituto de Investigación Sanitaria Princesa, Universidad Autónoma de Madrid, 28006 Madrid, Spain; [2]Department of Immunology, Hospital Universitario de la Princesa, Instituto de Investigación Sanitaria Princesa, Centro Nacional de Investigaciones Cardiovasculares Carlos III, Universidad Autónoma de Madrid, 28006 Madrid, Spain; [3]CIBER de Enfermedades Cardiovasculares (CIBERCV) and Centro Nacional de Investigaciones Cardiovasculares (CNIC), 28029 Madrid, Spain; [4]Sistemas Genómicos, 46980 Valencia, Spain; and [5]Neurosurgery & National Reference Unit for the Treatment of Refractory Epilepsy, Instituto de Investigación Sanitaria Hospital de la Princesa, 28006 Madrid, Spain

Context: Circulating microRNAs (miRNAs) are emerging as an interesting research area because of their potential role as novel biomarkers and therapeutic targets. Their involvement in autoimmune thyroid diseases (AITDs) has not been fully explored.

Objective: To compare the expression profile of miRNAs in thyroid tissue from patients with AITD and controls, using next-generation sequencing, further validated our findings in thyroid and serum samples.

Design: Twenty fresh-frozen thyroid tissues (15 from patients with AITD and 5 from controls) were used for miRNA next-generation sequencing. Thirty-six thyroid samples were recruited for the qRT-PCR validation test and 58 serum samples for further validation in peripheral blood.

Results: Expression of several miRNAs that had been previously associated with relevant immunological functions was significantly dysregulated. Specifically, eight differentially expressed miRNAs (miR-21-5p, miR-142-3p, miR-146a-5p, miR-146b-5p, miR-155-5p, miR-338-5p, miR-342-5p, and miR-766-3p) were confirmed using qRT-PCR in thyroid samples, and three had the same behavior in tissue and serum samples (miR-21-5p, miR-142-3p, and miR-146a-5p). Furthermore, when the expression of these miRNAs was assessed together with five additional ones previously related to AITD in peripheral blood, the expression of five (miR-Let7d-5p, miR-21-5p, miR-96-5p, miR-142-3p, and miR-301a-3p) was significantly expressed in AITD and, in patients with Graves disease (GD), was correlated with a higher severity of disease, including active ophthalmopathy, goiter, higher antibody titers, and/or higher recurrence rates.

Conclusions: The present findings identify a serum five-signature miRNA that could be an independent risk factor for developing AITD and a predisposition of a worse clinical picture in patients with GD. (***J Clin Endocrinol Metab*** **103: 1139–1150, 2018)**

ISSN Print 0021-972X ISSN Online 1945-7197
Printed in USA

Received 20 October 2017. Accepted 4 January 2018.
First Published Online 9 January 2018

Abbreviations: AITD, autoimmune thyroid disease; AUC, area under the curve; cDNA, complementary DNA; DE, differentially expressed; FFPE, formalin fixed, paraffin embedded; GD, Graves disease; GO, Graves ophthalmopathy; HT, Hashimoto thyroiditis; miRNA, microRNA; NGS, next-generation sequencing; PCR, polymerase chain reaction; qRT-PCR, quantitative reverse transcription polymerase chain reaction; ROC, receiver operating characteristic; Tg-Ab, antithyroglobulin antibody; TPO-Ab, antithyroid peroxidase antibody; TSHR-Ab, antithyrotropin receptor antibody.

Autoimmune thyroid disorders (AITDs) result from a dysregulation of the immune system directed against the thyroid and include a broad spectrum of diseases. The two main phenotypes of AITD, Hashimoto thyroiditis (HT) and Graves disease (GD), are both characterized by the presence of circulating thyroid antibodies and infiltration by autoreactive lymphocytes in the thyroid gland and sometimes the orbit. It has been traditionally thought that HT is mainly mediated by a cellular autoimmune response, whereas GD mainly has been considered to be mediated by a humoral response, mainly due to the presence of autoantibodies directed against the thyrotropin receptor [antithyrotropin receptor antibody (TSHR-Ab)], which lead to development of goiter and hyperthyroidism (1–3). Moreover, both immune responses, including TSHR-Ab, also have been reported in the pathogenesis of Graves ophthalmopathy (GO), one of the most common extrathyroid manifestations of AITD, which may occur clinically in up to 25% of patients with GD (4). The pathogenesis of AITD is probably related to a complex and multifactorial interplay of specific susceptibility genes and environmental exposures, leading to the breakdown of self-tolerance and subsequent development of autoimmune diseases.

MicroRNAs (miRNAs) are small non-protein-coding RNA molecules of ~22 nucleotides that interact with their targeted RNA in a sequence-dependent manner and therefore function as regulators of gene expression at a posttranscriptional level mainly by repressing the translation and also by decreasing target messenger RNA levels (5). Currently, nearly 3000 human miRNAs have been annotated in the miRBase (6). miRNAs have been recently involved in several biological processes, including immune functions, cellular apoptosis, cell differentiation and development, proliferation, and metabolism. The increasing importance of miRNAs highlights their potential role as biomarkers of disease and even their utility as therapeutic targets. In recent years, circulating miRNAs have been an interesting area of research due to their stability and reproducibility (7), and studies describing the role of miRNAs in the immune response and in autoimmune diseases have progressively developed. In this regard, evidence of differential miRNA expression has been reported in numerous immunological disorders such as rheumatoid arthritis, systemic lupus erythematosus, Sjögren disease, and psoriasis, among others (7–11).

Several reports have been published over the past years regarding the specific scenario of miRNAs and AITD with discordant results (12–27). These discrepancies can be attributed to the differences between the techniques used [microarray and/or quantitative reverse transcription polymerase chain reaction (qRT-PCR) assays], the materials analyzed (peripheral blood mononuclear cells, serum, plasma, thyrocytes, orbital fibroblasts, and thyroid tissue), the different preservation methods (frozen vs paraffin embedded), and the specific type of individual AITD evaluated (all AITD, HT, GD, or GO). However, none of these previous studies have analyzed miRNAs in fresh thyroid tissue, in the whole spectrum of AITD, using next-generation sequencing (NGS). The interest in this latter technique lies in the fact that, in comparison with microarrays, NGS has a greater ability to capture the scale and complexity of whole transcriptomes. Furthermore, NGS allows the discovery of novel miRNAs and can identify miRNAs that are expressed at levels that fall below microarrays' detectable threshold. In this study, therefore, we aimed to identify differentially expressed (DE) miRNAs in AITD thyroid tissue samples in comparison with controls by means of NGS and then corroborated their expression in serum samples. We then correlated their expression with patients' clinical data to identify potential diagnostic biomarkers and therapeutic targets of the disease.

Materials and Methods

Patients

Fresh-frozen thyroid tissue samples from 26 patients with AITD (9 with HT, 7 with GD without GO, and 10 with GD and GO) and 10 controls were collected. In addition, we collected formalin-fixed, paraffin-embedded (FFPE) samples from 19 patients with AITD (7 with HT, 6 with GD without GO, and 6 with GD and GO), of which 11 were the same as the frozen tissue, and 6 were healthy controls. Concomitantly, we also evaluated serum samples from 36 patients with AITD (14 with HT, 10 with GD without GO, and 12 with GD with GO) and 22 healthy controls. Clinical diagnoses were all reviewed by a single experienced endocrinologist; established on commonly accepted clinical, laboratory, and histological criteria (2); and based on information collected from clinical records (Tables 1 and 2). More details of clinical data are available in the Supplemental Material and Methods.

The project was approved by the Internal Ethical Review Committee of the Hospital de la Princesa, and written informed consent was obtained from all patients prior to inclusion, in accordance with the Declaration of Helsinki.

Tissue and serum samples

All thyroid tissues were obtained from surgical thyroidectomies performed in our hospital and reviewed by an experienced pathologist. Samples were immediately snap-frozen in liquid nitrogen–cooled isopentane and transferred to a −80°C freezer for long-time preservation or processed by the Department of Pathology to create FFPE tissues. Serum samples were isolated by centrifugation (1500 × *g*) from 10 mL of total blood and stored at −80°C until use.

Tissue miRNA isolation

RNA was isolated from 36 fresh-frozen thyroid tissues: 20 samples were used for miRNA NGS and all 36 for the qRT-PCR

Table 1. Clinical Features of Patients With AITD From Whom Thyroid Tissue Was Collected

Characteristic	HT (n = 9)	GD (n = 17)	Controls (n = 10)
Sex, female/male	9/0	15/2	7/3
Age, y	63 (50.5–71.5)	39 (29.5–52.5)	43 (32.2–51.8)
TSH, μU/mL	2.3 (1–8.5)	1.8 (0.2–9.5)	0
FT4, ng/dL	1.1 (0.9–1.2)	1.1 (0.8–1.3)	0
Tg-Ab, UI/mL	311 (213–382.3)	456 (20–1103)	0
TPO-Ab, UI/mL	150 (20–306)	102 (43.2–635.5)	0
TSHR-Ab, U/L	0.5 (0.5–0.5)	5.6 (1.7–17.5)	0

Values show number for categorical values and median (25th to 75th interquartile intervals) for continuous variables. FT4, free thyroxine (normal range, 0.93 to 1.7 ng/dL); Tg-Ab (negative <344 UI/mL); TPO-Ab (negative <100 UI/mL); TSH, thyrotropin (normal range, 0.27 to 4.20 mU/mL); TSHR-Ab (negative <0.7 U/L).

validation test. Total RNA was isolated using miRNeasy Mini Kit (Qiagen, Germantown, MD), according to the manufacturer's instructions. The quality and quantity of RNA and miRNA were assessed in a 2100 Bioanalyzer by using a RNA 6000 Nano kit and a Small RNA kit (Agilent Technologies, Palo Alto, CA). For the study, only those samples with an RNA integrity number >7 were included. To empower the statistical analysis, we isolated miRNA from 25 FFPE samples, 12 of which were repeated from frozen samples to verify their quality and reproducibility. FFPE samples were isolated using the miRneasy FFPE Mini kit (Qiagen).

Serum miRNA isolation

To test hemolysis in serum samples, the absorbance of free hemoglobin at 414 nm was measured. Those samples with a peak >0.2 were discarded. miRNA from serum samples were isolated using miRCURY RNA Isolation Kit Biofluids (Exiqon, Vedbaek, Denmark), according to the manufacturer's instruction. A mixture containing 1.25 μg/mL MS2 bacteriophage RNA and RNA spike-ins (UniSp2, UniSp4, and UniSp5) was added to 200 μL serum. RNA was purified on a miRNA mini-spin column BF, eluted in 50 μL RNase-free water, and stored at −80°C. The robustness of the RNA isolation process and the quality of isolated miRNA were assessed using miRCURY microRNA QC Panels (Exiqon).

miRNA NGS

NGS of 20 thyroid samples (5 controls, 5 with HT, 5 with GD without GO, and 5 with GD with GO) was performed on the Illumina platform (HiSEquation 2000; Illumina, San Diego, CA) at Sistemas Genómicos (Valencia, Spain). The procedure included the following steps/phases: (1) Quality control of RNA: the quality and the quantity of RNA were determined in a Bioanalyzer 2100 Small RNA assay and Qubit 2.0 fluorometer. (2) Preparation of libraries: complementary DNA (cDNA) libraries were obtained following Illumina's recommendations. Briefly, 3′ and 5′ adaptors were sequentially ligated to the RNA prior to reverse transcription and cDNA generation. cDNA was enriched with polymerase chain reaction (PCR) to create the indexed double-stranded cDNA library. Size selection was performed using 6% polyacrylamide gel. The quality of the libraries was analyzed using Bioanalyzer 2100, High Sensitivity assay, and the quantity of the libraries was determined by real-time PCR in Light Cycler 480 (Roche Farma, Madrid, Spain). (3) Equimolar pooling of libraries was performed before proceeding to the generation of clusters in cbot (Illumina). The pool of the cDNA libraries was sequenced by paired-end sequencing (100 × 2) in the Illumina HiSEquation 2000 sequencer. The bioinformatic analysis of NGS and raw data availability is described in Supplemental Material and Methods.

Reverse transcription and qRT-PCR of tissue and serum samples

First-strand cDNA was generated using a cDNA synthesis kit, and subsequent qRT-PCR was performed in triplicate using miRCURY LNA Universal RT microRNA PCR ExiLENT SYBR Green (both from Exiqon) with the CFX384 Touch Real-Time PCR Detection System (Bio-Rad, Alcobendas, Madrid).

Table 2. Clinical Features of Patients With AITD From Whom Serum Was Collected

	HT (n = 14)		GD (n = 22)		
Characteristic	Euthyroid (n = 8)	Hypothyroid (n = 6)	Hyperthyroid (n = 15)	Hypothyroid (n = 7)	Controls (n = 22)
Sex, female/male	6/2	4/2	11/4	7/0	9/13
Age, y	47 (31.2–62.7)	39 (28.5–54.2)	45 (30–54)	46 (41–54)	31 (25.5–40)
Ophthalmopathy	0	0	8	4	0
TSH, μU/mL	2.5 (1.5–2.9)	10.7 (4.9–23.9)	0	6.55 (3.21–23.96)	—
FT4, ng/dL	1.2 (0.9–1.3)	1.2 (0.9–1.4)	3 (1.9–4.5)	0.61 (0.36–1)	—
Tg-Ab, UI/mL	0 (0–986.8)	398 (0–1198)	0 (0–764)	0 (0–70.2)	0
TPO-Ab, UI/mL	424 (126.3–844.8)	252 (0–669.5)	156 (0–542.8)	98.6 (0–273)	0
TSHR-Ab, U/L	0.2 (0–1.1)	0 (0–0.8)	3.4 (1.9–5.6)	3.56 (1.66–6.3)	0.01 (0–0.07)

Values show number for categorical values and median (25th to 75th interquartile intervals) for continuous variables. FT4, free thyroxine (normal range, 0.93 to 1.7 ng/dL); Tg-Ab (negative <344 UI/mL); TPO-Ab (negative <100 UI/mL); TSH, thyrotropin (normal range, 0.27 to 4.20 mU/mL); TSHR-Ab (negative <0.7 U/L).

Expression of miRNAs was performed using miRNA LNA PCR primer sets (Exiqon). Expression stabilities of the reference genes were evaluated using geNorm (28), NormFinder (29), and the coefficient of variation score described by Marabita *et al.* (30). Data were normalized using the geometric mean Ct of the best gene combination generated by the algorithms (Supplemental Table 1 and Supplemental Fig. 1). Relative expression was determined using the log base 2 values of the difference Cts between miRNAs and the geometric mean of the selected housekeeping genes. See Supplemental Material and Methods for detailed technical descriptions of the normalization.

Statistical analysis

Descriptive results were expressed as mean ± standard deviation, mean ± error of the mean, or median and 25th to 75th percentiles, as appropriate. Spearman bivariate correlations were performed for all quantitative variables and differences between groups were compared using analysis of variance (Mann-Whitney *U* or Kruskal-Wallis analysis of variance, as appropriate). A logistic regression model was used to determine the differences in each normalized miRNA between controls and AITD groups, adjusted by age and sex, as recommended in previous reports (31). Receiver operating characteristic (ROC) curve analyses were performed to assess the classification power of each logistic regression model. Samples from all groups within an experiment were processed at the same time. The *P* values were two-sided, and statistical significance was considered when $P < 0.05$. Data are presented with the following specific *P* values: $P < 0.05$, $P < 0.01$, and $P < 0.001$. All statistical analyses were performed using GraphPad Prism 4 software (GraphPad Software, La Jolla, CA) and STATA (StataCorp LLC, College Station, TX).

Results

miRNA expression in patients with AITD

Unsupervised hierarchical clustering and principal component analysis were used to investigate the potential identification of AITD subgroups, based on their molecular expression profile. We performed NGS using RNA obtained from thyroids from five patients with HT, five patients with GD with no GO, five patients with GD with GO, and five healthy participants. The analysis revealed a slightly but not substantial separation between AITD groups. Control samples clustered together and formed a separate subcluster, indicating that these samples have a very similar miRNA signature and that this signature was different from those of AITD samples. Regarding the principal component analysis, an outlier sample from the GD group was detected and excluded from the study (Fig. 1A and 1B). We, therefore, decided to assess the differential miRNA expression of all AITD samples together in the same group, in comparison with the control group. A total of 3431 sequences were detected. In particular, 19 miRNAs were upregulated and 1 was downregulated more than twofold in AITD vs normal thyroid. Of these, miR-146b-5p displayed the most significant upregulation, with a log twofold change of 6.303 and $P < 0.00001$.

Gene ontology enrichment of differentially expressed miRNAs

To evaluate the association of miRNAs with relevant immunological functions, target genes biologically annotated for the DE miRNAs were identified using miRTarBase and TargetScan. Gene ontology–selected immunological enriched processes were associated with DE miRNAS (Fig. 1C and Supplemental Table 2). The analysis of biological network exploration showed the correlation and cooperation of miRNAs related to the immunological system (Supplemental Fig. 2). In fact, we can observe the cooperation of pathway reactions relative to the immune and adaptive system of miR-96-5p, miR-142-3p, miR-146a-5p, and miR-146b-5p. At the same time, miR-21-5p and miR-6503-3p cooperate with miR-146a-5p in processes related to the Toll-like receptor and interferon signaling pathways, respectively. Considering this, 10 top-ranked selected miRNAs importantly associated with immune pathways were selected for validation by qRT-PCR: miR-21-5p, miR-96-5p, miR-142-3p, miR-146a-5p, miR-146b-5p, miR-155-5p, miR-338-5p, miR-342-5p, miR-766-3p, and miR-6503-3p (Fig. 1D).

Validation of significant differentially expressed miRNAs in thyroid tissue

To validate the top-ranked DE selected miRNAs, qRT-PCR was performed in 36 fresh-frozen and 25 FFPE thyroid tissue from the same samples. There was a good correlation in 5 of 10 miRNAs in the same samples extracted from fresh-frozen and FFPE tissues ($P < 0.05$) (Supplemental Fig. 3). In this context, we decided to exclude FFPE samples from the study and continue only with the expressions related to frozen samples.

Then, comparison of the expression levels performed between NGS data and qRT-PCR in frozen tissues demonstrated a similar expression pattern between both methods (Fig. 2A). Of the top 10 selected miRNAs, 8 were confirmed to be DE in AITD samples (miR-21-5p, $P < 0.01$; miR-142-3p, $P < 0.01$; miR-146a-5p, $P < 0.001$; miR-146b-5p, $P < 0.001$; miR-155-5p, $P < 0.05$; miR-338-5p, $P < 0.05$; miR-342-5p, $P < 0.001$; and miR-766-3p, $P < 0.001$). However, although there was a trend toward being increased in AITD, no significant differences were found for miR-96-5p and miR-6503-5p between the two groups (Fig. 2B).

Expression of identified thyroid DE miRNAs in serum samples

We then determined whether the selected DE miRNAs were detected in serum samples of 8 patients with active

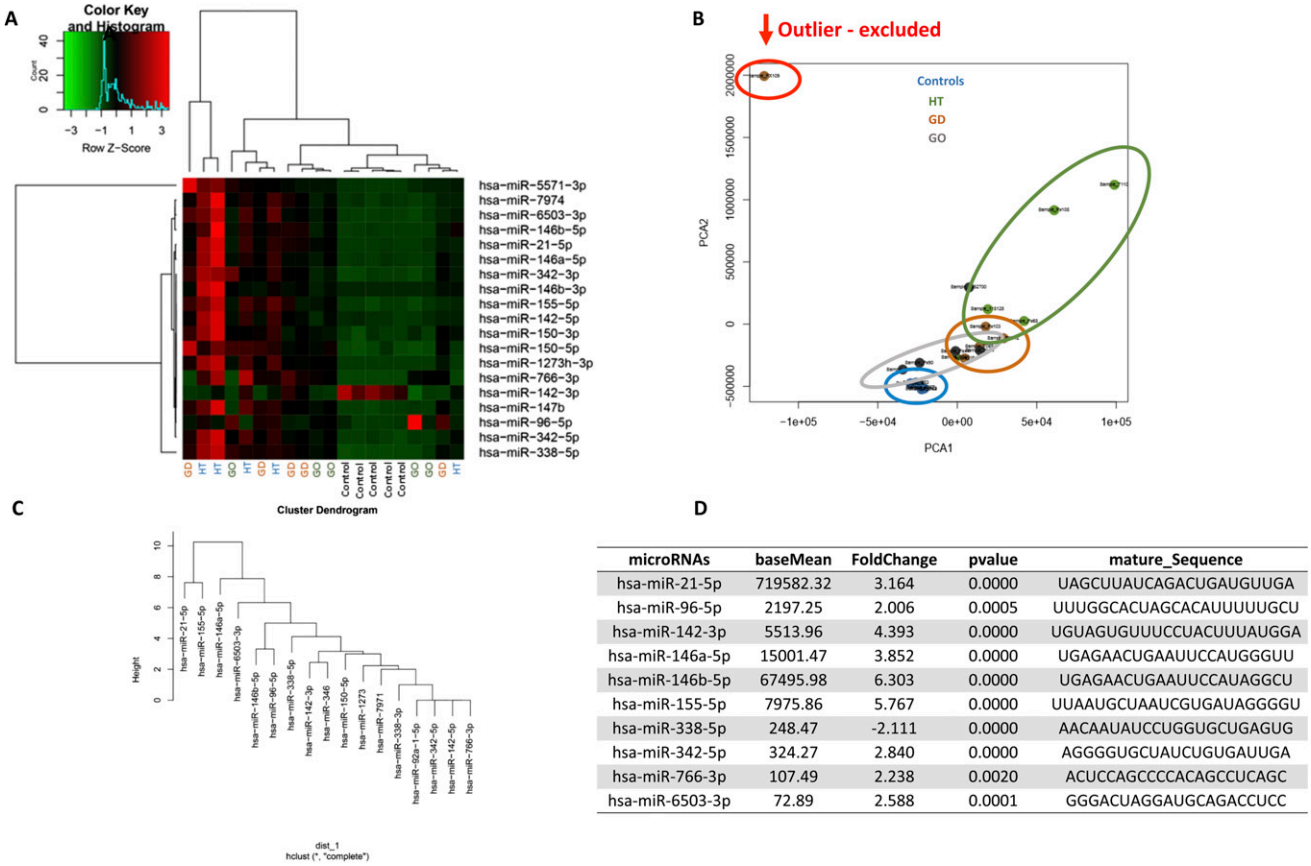

microRNAs	baseMean	FoldChange	pvalue	mature_Sequence
hsa-miR-21-5p	719582.32	3.164	0.0000	UAGCUUAUCAGACUGAUGUUGA
hsa-miR-96-5p	2197.25	2.006	0.0005	UUUGGCACUAGCACAUUUUUGCU
hsa-miR-142-3p	5513.96	4.393	0.0000	UGUAGUGUUUCCUACUUUAUGGA
hsa-miR-146a-5p	15001.47	3.852	0.0000	UGAGAACUGAAUUCCAUGGGUU
hsa-miR-146b-5p	67495.98	6.303	0.0000	UGAGAACUGAAUUCCAUAGGCU
hsa-miR-155-5p	7975.86	5.767	0.0000	UUAAUGCUAAUCGUGAUAGGGGU
hsa-miR-338-5p	248.47	-2.111	0.0000	AACAAUAUCCUGGUGCUGAGUG
hsa-miR-342-5p	324.27	2.840	0.0000	AGGGGUGCUAUCUGUGAUUGA
hsa-miR-766-3p	107.49	2.238	0.0020	ACUCCAGCCCCACAGCCUCAGC
hsa-miR-6503-3p	72.89	2.588	0.0001	GGGACUAGGAUGCAGACCUCC

Figure 1. (A) Heatmap hierarchical clustering of DE miRNAs in AITD tissue samples on the basis of 19 DE miRNAs. The graph shows miRNA expression in thyroid tissue from AITD samples compared with controls, expressed in fold change. The key color bar indicates that miRNA expression levels increased from green to red, depending on the fold change. (B) Principal component analysis (PCA) projected as a two-dimensional scatterplot. The most correlated samples are circled in different colors (blue = controls, green = HT, brown = GD, and gray = GO). Circled in red is an outlier that was excluded from the analysis (see text for full explanation). (C) Cluster dendrogram of miRNAs that have been associated by immunological enrichment analysis (false discovery rate <0.05). miR-21-5p, miR-155-5p, and miR-146a-5p are the most associated with immunological pathways. (D) Top 10 dysregulated miRNAs in AITD samples selected for validation by qRT-PCR ($P < 0.05$) and fold change ± 2 calculated using the algorithm DESeq2; base mean indicates the mean of reads of the miRNAs adjusted by the mean of the total reads generated in the NGS.

GO and 4 patients with inactive GO, 10 patients with GD with no GO, 14 patients with HT, and 22 healthy controls. In addition to the 10 DE miRNAs identified in thyroid tissue samples, 5 other miRNAs involved in immune functions or identified in previous studies were also included for validation in AITD serum samples (miR-Let7d-5p, miR-142-5p, miR-126-3p, miR-223-3p, and miR-301a-3p) (24, 32–34). Eight of this whole set of miRNAs analyzed were DE in AITD samples (miR-Let7d-5p, $P < 0.001$; miR-21-5p, $P < 0.0001$; miR-96-5p, $P < 0.001$; miR-142-3p, $P < 0.01$; miR142-5p, $P < 0.001$; miR146a-5p, $P < 0.05$; miR-301a-3p, $P < 0.001$; and miR-6503-3p, $P < 0.05$) (Fig. 2B). All were upregulated in AITD, except for miR-Let-7d, which was downregulated. To discriminate if these miRNAs were dysregulated according to the type of AITD (HT or GD), we analyzed the levels of DE miRNAs in each subgroup; miR-Let7d-5p was DE in HT, mir-142-3p in GD, and miR-21-5p, miR-96-5p, and miR-301-3p in both HT and GD. Although miR-146a-5p and miR-6503-3p lost significance when both groups were considered separately, we observed the same trend of dysregulation in all of them, denoting the distinction between controls and HT/GD (Fig. 2C and Fig. 3A).

A five-signature miRNA to discriminate patients with AITD vs controls: correlation with clinical features

To assess the existence of any possible associations between miRNA levels and clinical features and explore their clinical utility, we first investigated the correlations of all the analyzed miRNAs with patients' corresponding serum levels of free thyroxine, thyrotropin, antithyroid peroxidase antibody (TPO-Ab), antithyroglobulin antibody (Tg-Ab), and TSHR-Ab (correlation heatmap in Fig. 4A). Spearman ρ analyses revealed that miR-Let7d-5p was negatively associated with levels of TPO-Ab ($r = -0.38$), whereas miR-21-5p and miR-96-5p were

A

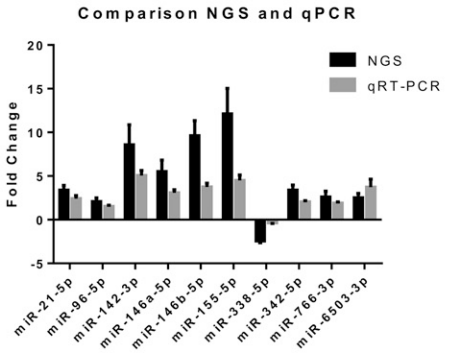

B

miRNA	Tissue samples		Serum samples	
	p-Value	Significance ($P < 0.05$)	*p*-Value	Significance ($P < 0.05$)
miR-21-5p	0.0029	Yes	<0.0001	Yes
miR-96-5p	0.063	No	0.0003	Yes
miR-142-3p	0.001	Yes	0.0012	Yes
miR-146a-5p	0.0004	Yes	0.0462	Yes
miR-146b-5p	0.0006	Yes	0.4298	No
miR-155-5p	0.0153	Yes	0.776	No
miR-338-5p	0.038	Yes	0.6473	No
miR-342-5p	0.001	Yes	0.2213	No
miR-766-3p	0.0063	Yes	0.0699	No
miR-6503-3p	0.5288	No	0.049	Yes
Let7d-5p			0.0032	Yes
miR-126-3p			0.3006	No
miR-142-5p			0.0022	Yes
miR-223-3p			0.4581	No
miR-301a-3p			0.0037	Yes

C

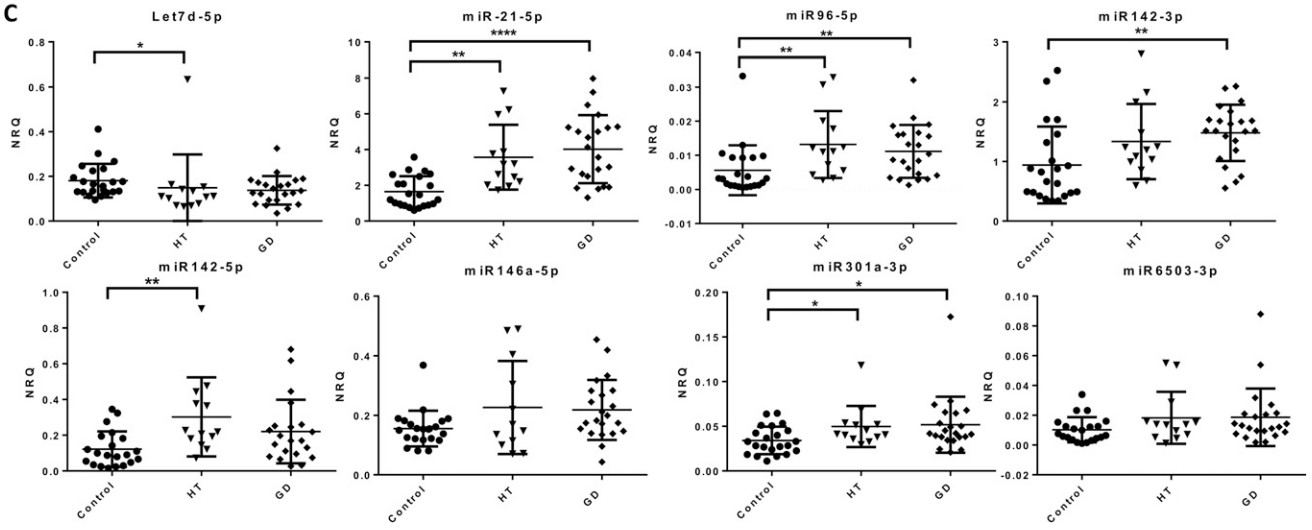

Figure 2. (A) Comparison of miRNA expression between NGS and qRT-PCR. miRNAs determined to be DE in patients with AITD by NGS were validated by qRT-PCR. The height of the columns in the chart represents the log-transformed average fold change in expression, comparing the expression levels of AITD samples with normal thyroid tissues for each of the validated miRNAs. A total of 10 miRNAs were selected for validation, and 8 were confirmed by qRT-PCR. Data are expressed as mean ± standard error of the mean. (B) miRNAs in the validation study in tissue and serum samples. Eight different miRNAs were DE in 26 patients with AITD compared with 10 controls measured in fresh-frozen thyroid tissue samples (miR-21-5p, miR-142-3p, miR-146a-5p, miR-146b-5p, miR-155-5p, miR-338-5p, miR-342-5p, and miR-766-3p). Of the total circulating miRNAs evaluated in 56 samples (36 patients with AITD and 22 healthy controls), miR-21-5p, miR-96-5p, miR-142-3p, and miR-146a-5p were DE in patients with AITD vs controls. Furthermore, of the five miRNAs included in the study, miR-Let7d-5p, miR-142-5p, and miR-301a-3p were also DE in serum samples. (C) Normalized relative quantities (NRQs) of miRNAs in serum samples analyzed according to the different subgroups of AITD: HT and GD. miR-Let7d-5p was DE in HT, mir-142-3p in GD, and miR-21-5p, 96-5p, and 301-3p in both HT and GD. miR146a-5p and miR-6503-3p lost significance when we distinguished between HT and GD. Data are presented as mean ± standard deviation. $^{*}P < 0.05$. $^{**}P < 0.01$. $^{***}P < 0.001$. $^{****}P = 0.0001$.

positively correlated with TPO-Ab ($r = 0.39$ and $r = 0.48$, respectively), Tg-Ab ($r = 0.36$ and $r = 0.4$, respectively), and TSHR-Ab ($r = 0.45$ and $r = 0.4$, respectively). miR-142-3p and miR-301a-3p were only positively associated with TSHR-Ab ($r = 0.38$ and $r = 0.31$), and miR-6503-3p correlated with TPO-Ab ($r = 0.27$). Interestingly, these miRNAs (except for miR-6503-3p) were DE in HT and/or GD. Also, all miRNAs were significantly correlated between themselves, with a remarkable similarity between miR-21-5p and miR-96-5, which exhibited an analogous behavior regarding their correlation with clinical features (Fig. 4B).

We assessed the discriminating potency between AITD and controls of these circulating miRNAs using ROC curve analyses (Fig. 4C), and we confirmed that five miRNAs (miR-Let7d-5p, miR-21-5p, miR-96-5p, miR-142-3p, and miR-301a-3p) were good discriminators [area under the curve (AUC) ≥0.848, with >76% correctly classified instances]. Then, we assessed the prognostic role of miRNAs in GD by correlating DE miRNAs of the signature with clinical parameters, including persistent and/or severe forms of hyperthyroidism. Relative expression of miR-Let7d-5p, miR-96-5p, and miR-301a-3p was significantly different in patients with GO than in controls ($P = 0.0073$, $P = 0.0055$, and $P = 0.0374$, respectively), although no differences were found between controls and patients with GD without GO ($P > 0.99$, $P = 0.06$, and $P = 0.42$, respectively) (Fig. 5A). However,

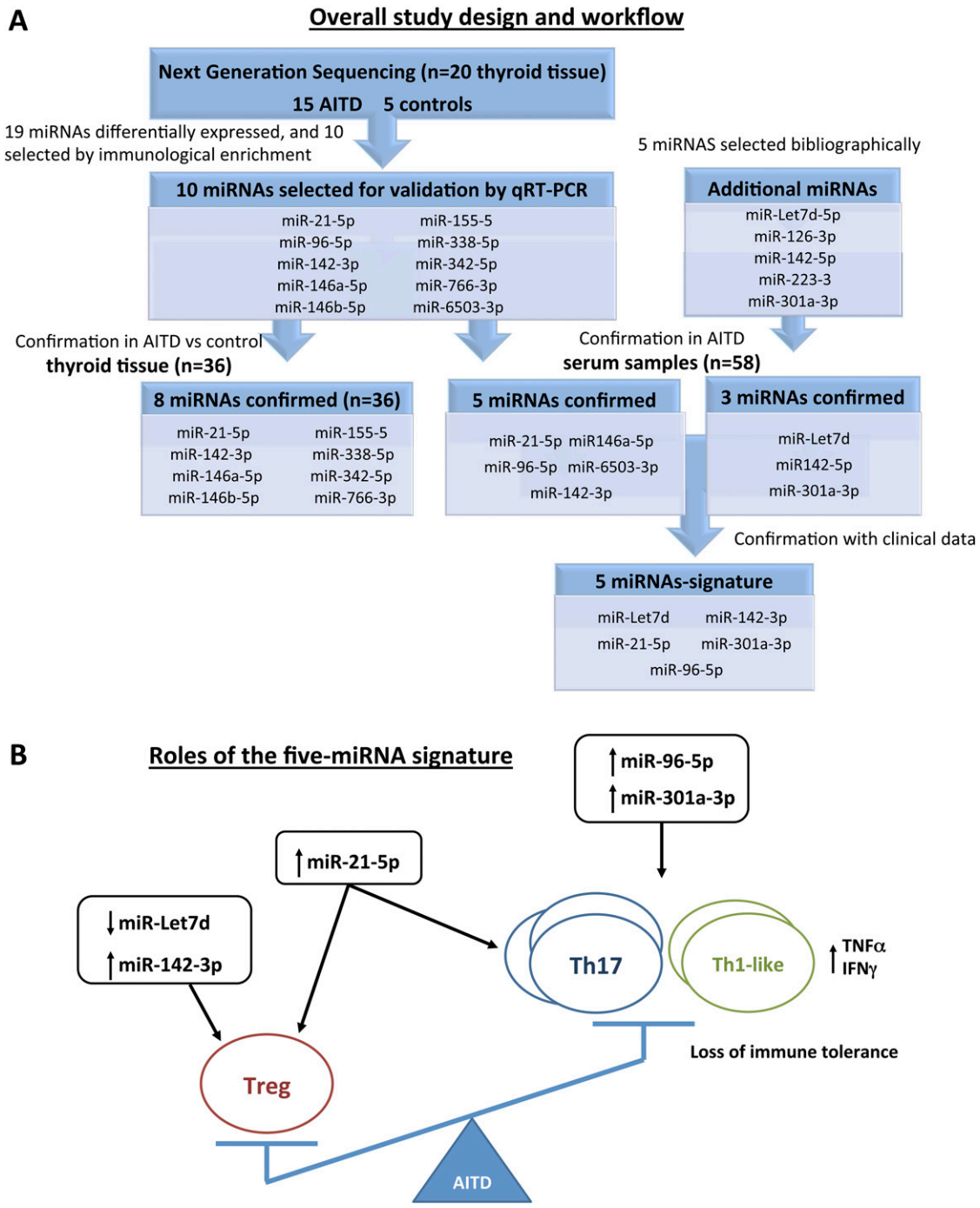

Figure 3. (A) Overall study design and workflow. NGS was performed in 20 thyroid tissues. Ten miRNAs were selected for validation by qRT-PCR, and 8 were confirmed. In five cases, miRNAs from NGS were confirmed in serum samples. Five additional miRNAs were selected bibliographically. Of the 15 miRNAs studied in serum samples (10 from NGS and 5 selected bibliographically), 5 were confirmed as a specific miRNA signature. (B) Roles of the five-signature miRNA (miR-Let7d-5p, miR-21-5p, miR-96-5p, miR-142-3p, and miR-301a-3p) found in AITD samples. The lower levels of miR-Let7d-5p fall to the suppression of Th1 cells by Treg cells, leading to Th1 cell proliferation and interferon-γ (IFN-γ) secretion (32). The increase of miR-142-3p could impair the inhibitory effect of Treg cells on the proliferative response and cytokine production of CD4+CD25− T cells (35). miR-21-5p can regulate the Th1/Th2 balance and promote Th17 differentiation by inhibiting Smad-7 (36). miR-96-5p can increase cytokine production of Th17 cells (37). miR-301a-3p can downregulate PIAS3, promoting Th17 development (34). The altered expression of all these miRNAs can alter the normal function of immune cells, leading to a loss of immune tolerance in AITD. TNFα, tumor necrosis factor α.

miR-Let7d-5p was significantly lower in patients with GO compared with patients with GD without GO ($P = 0.016$) and more remarkably in those with active GO ($P = 0.0016$) (Fig. 5B), which also had a negative correlation with clinical activity score ($r = -0.6504$, $P = 0.0014$) (Fig. 5C). Patients with more severe disease had lower miR-Let7d-5p levels ($P = 0.034$) (Fig. 5D). For miR-21-5p, a higher expression was significantly correlated with a worse prognosis, with more

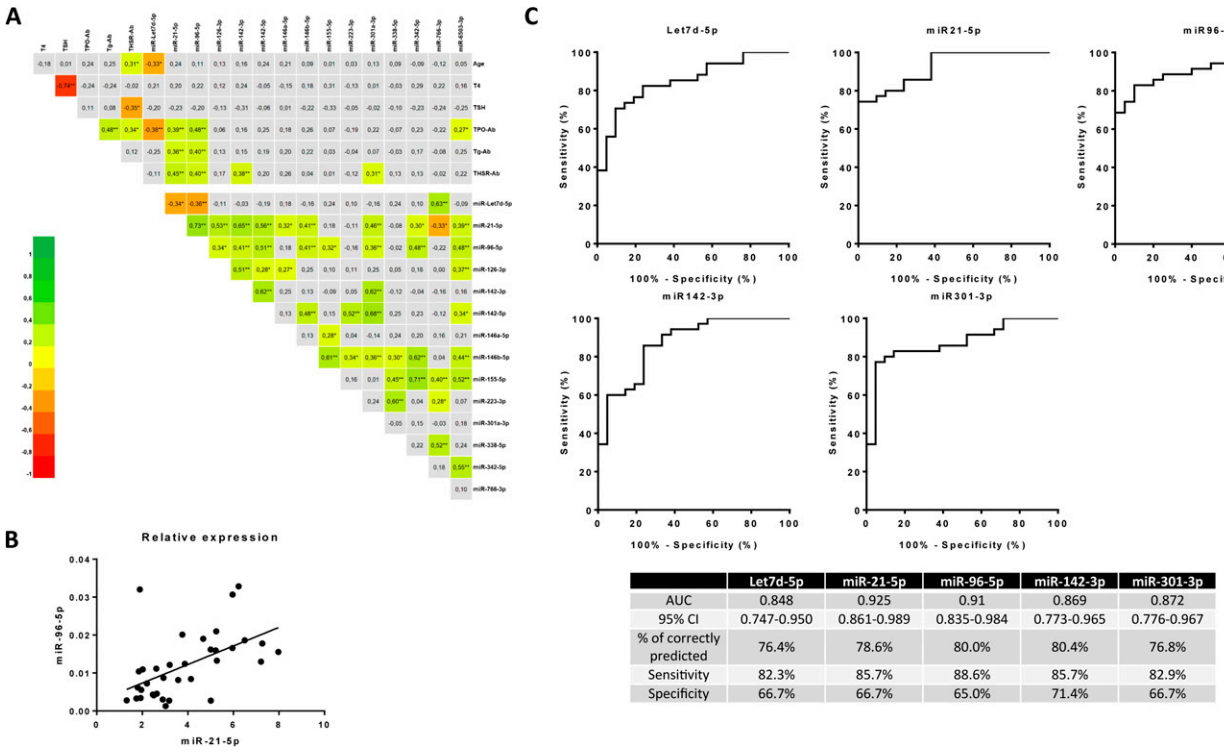

	Let7d-5p	miR-21-5p	miR-96-5p	miR-142-3p	miR-301-3p
AUC	0.848	0.925	0.91	0.869	0.872
95% CI	0.747-0.950	0.861-0.989	0.835-0.984	0.773-0.965	0.776-0.967
% of correctly predicted	76.4%	78.6%	80.0%	80.4%	76.8%
Sensitivity	82.3%	85.7%	88.6%	85.7%	82.9%
Specificity	66.7%	66.7%	65.0%	71.4%	66.7%

Figure 4. (A) Correlation heatmap between the expression of miRNAs and clinical and laboratory parameters (Spearman ρ analysis). Significant negative correlations are shown in red and significant positive correlations in green ($*P < 0.05$; $**P < 0.01$). Bottom left triangle shows correlations between miRNAs and top square shows correlations between miRNAs and clinical data. miR-Let7d-5p is negatively associated with levels of TPO-Ab ($r = -0.38$). miR-21-5p and miR-96-5p are positively correlated with TPO-Ab ($r = 0.39$ and $r = 0.48$, respectively), Tg-Ab ($r = 0.36$ and $r = 0.4$ respectively), and TSHR-Ab ($r = 0.45$ and $r = 0.4$ respectively). miR-142-5p and miR-301a-3p are positively associated with TSHR-Ab ($r = 0.38$ and $r = 0.31$), and miR-6503-3p correlates with TPO-Ab ($r = 0.27$). (B) Correlation analysis between miR-21-5p and miR-96-5p ($r = 0.58$ and $P < 0.001$). (C) ROC curve analyses performed to assess the diagnostic value of circulating miR-Let7d-5p, miR-21-5p, miR-96-5p, miR-142-3p, and miR-301-3p to discriminate between controls and patients with AITD. The table shows the AUC, the percentage of correctly predicted instances, 95% confidence intervals (95% CIs), sensitivity, and specificity of the analyses.

patients presenting recurrent disease ($P = 0.028$) (Fig. 5E and Supplemental Table 3). In fact, after adjusting for age, sex, and TSHR-Ab, miR-21-5p remained significant ($P = 0.042$). Subsequent analysis using the method of all possible equations showed that combining miR-21-5p and TSHR-Ab in the regression model achieved the best predictive value for disease persistence. In this regard, ROC curves for miR-21-5p, TSHR-Ab, and a composite model of both markers (Fig. 5F) found that baseline miR-21-5p alone had an AUC of 0.85 and a percentage of correctly classified instances of 85%, whereas baseline TSHR-Ab alone had an AUC of 0.64 and a prediction of 65% at the cut point of 3. The composite marker had an AUC of 0.92 and a percentage of prediction of 90%.

Discussion

Accumulating evidence suggests that miRNAs can be used as biomarkers of various diseases, including various autoimmune disorders (38). In addition to tissue-derived miRNAs, circulating miRNAs, which are protected from endogenous RNase activity, are specific and stable and can be used as extracellular biomarkers. The advantage of using circulating miRNAs is that the diagnostic approach could be minimized to a single blood sample (7). Although studies have investigated miRNAs in patients with AITD, few have explored their clinical and diagnostic utility and their role in risk stratification.

In this study, we describe the global patterns of miRNA expression found in AITD thyroid samples. We found a good correlation between the expression profiles using NGS and qRT-PCR in fresh-frozen thyroid tissues, suggesting that NGS could be a reliable method for miRNA profiling in AITD. In fact, using NGS, we selected 10 miRNAs in accordance to immune pathways (cytokine signaling, Toll-like receptor cascade, interferon signaling, B-cell receptor signaling) and confirmed that 8 miRNAs were DE in the thyroid and 3 (miR-21-5p, miR-142-3p, and miR-146a-5p) in serum samples of patients with AITD. These results suggest that some of these circulating miRNAs are synthetized in thyroid tissue and are then released to human body fluids, including the blood, as a form of intercellular communication, so they could be used to monitor the altered tissue.

Some of the miRNAs found in the thyroid (miR-21-5p, miR-146a-5p, and miR-155-5p) have been widely reported

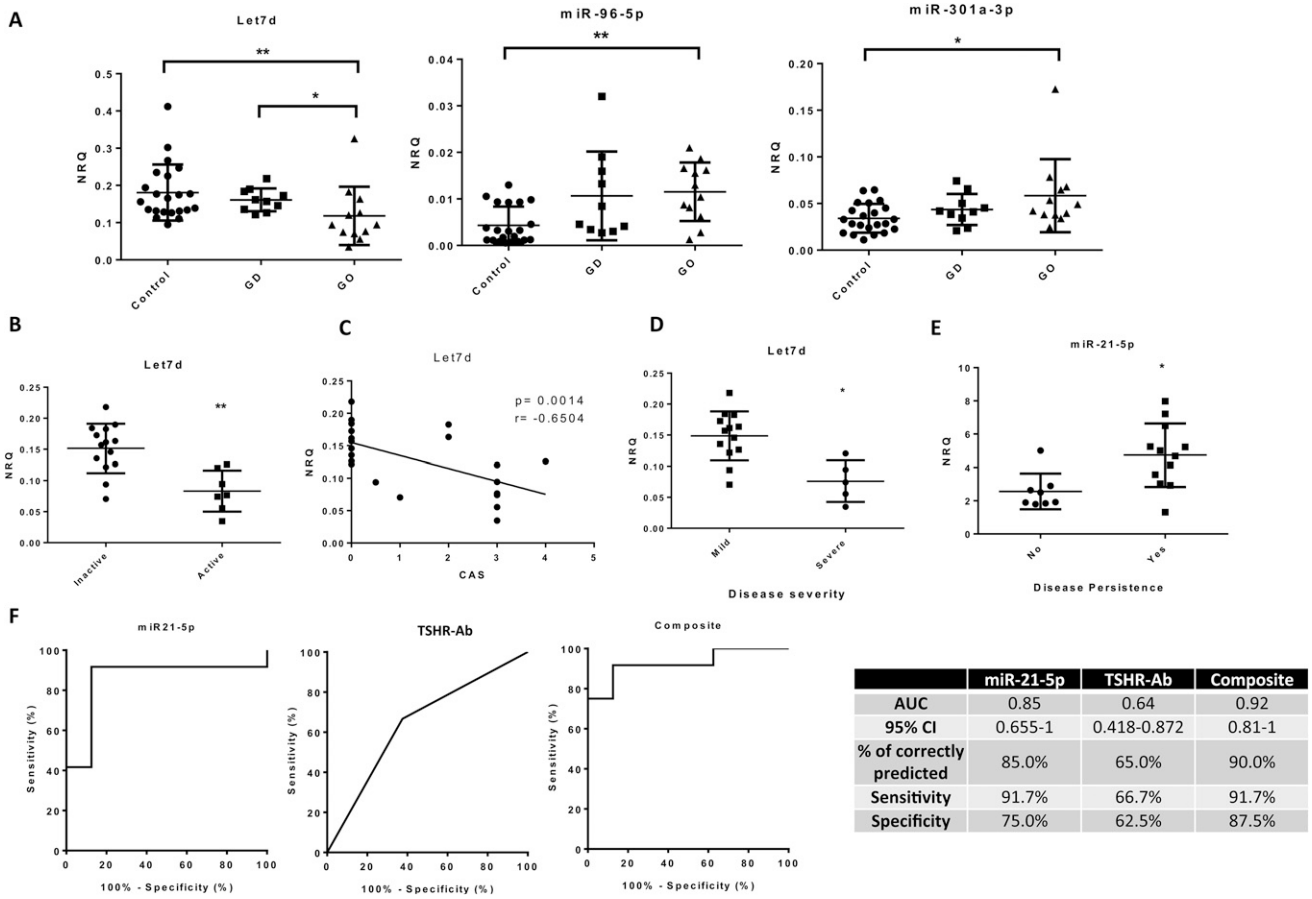

	miR-21-5p	TSHR-Ab	Composite
AUC	0.85	0.64	0.92
95% CI	0.655-1	0.418-0.872	0.81-1
% of correctly predicted	85.0%	65.0%	90.0%
Sensitivity	91.7%	66.7%	91.7%
Specificity	75.0%	62.5%	87.5%

Figure 5. Correlation of levels of miRNAs with clinical data of patients with GD. (A) Classification of patients with GD according to the presence or absence of GO. Relative expression of miR-Let7d-5p, miR-96-5p, and miR-301-3p was DE in the GO group compared with controls. In addition, miR-Let7d-5p was DE between patients with GD with and without GO. (B) The expression levels of miR-Let7d-5p were DE in patients with GD with active GO [clinical activity score (CAS) >3]. (C) There was a negative correlation between the expression of miR-Let7d-5p and CAS. (D) Levels of miR-Let7d-5p according to disease severity; patients with severe disease had lower levels of miR-Let7d-5p. (E) miR-21-5p was higher in patients with persistent disease. (F) ROC curves were performed to analyze the predictive values of regression models for disease persistence based on miR-21-5p, TSHR-Ab, and the composite of both parameters. Table shows the AUC, the percentage of correctly predicted instances, 95% confidence intervals (95% CIs), sensitivity, and specificity of the analyses. Data are presented as mean ± standard deviation. $*P < 0.05$. $**P < 0.01$. $***P < 0.001$. $****P = 0.0001$.

to participate in lymphocyte differentiation and activation (36, 39–43). For instance, miR-146 has been associated with regulation of the immune response (39, 41, 43) and miR-155 to T-regulatory cell development and Th17 differentiation (40, 42). Regarding AITD, studies on these miRNAs have been discordant, with reports of decreased or increased expression of miR-21-5p, miR-146a-5p, and/or miR-155-5p, depending on the specific type of disease (AITD vs HT vs GD), the tissue studied (thyroid tissue, needle aspiration samples, peripheral blood mononuclear cells, microvesicles, and/or serum), or the conservation method used (fresh samples vs FFPE) (12, 13, 20–22, 24, 44), hence the importance of studying homogeneous groups of patients, samples, and preservation methods. In our study, we found some differences in DE miRNAs when we analyzed AITD as a whole or as subgroups or in thyroid vs serum samples. Moreover, there was a poor correlation between the relative expression of miRNA in formalin-fixed and frozen samples, which forced us to exclude FFPE samples from our analysis to provide more robustness to our results (45–48). Taken together, all these issues could potentially explain the discrepancies observed between previous publications and our current findings.

To further evaluate if these miRNAs could behave as biomarkers of risk for developing AITD, we studied the top 10 miRNAs found in NGS and 5 additional miRNAs (miR-Let7d-5p, miR-126-3p, miR-142-5p, miR-223-3p, and miR-301a-3p), which have been previously reported to be involved in different autoimmune disorders, including AITD (24, 32–34). We found a good correlation between some of these miRNAs and all three thyroid autoantibody levels. Because these autoantibodies are frequently used to establish the risk of AITD, we assessed whether miRNAs could be also used in the same way. To do so, we performed a composite marker by a logistic regression model and found that a specific five-serum miRNA

signature (miR-Let7d-5p, miR-21-5p, miR-96-5p, miR-142-3p, and miR-301-3p) was able to assign a risk for developing AITD independently of autoantibody titers.

We also evaluated if this signature could be the used in the clinical evaluation of patients with GD. We found that three of the signature's miRNAs (miR-Let7d-5p, miR-96-5p, and miR-301-3p) were DE in patients with GO, whereas miR-Let7d-5p was inversely correlated with a higher GD severity and GO clinical activity. In this regard, as miR-Let7 has a specific Treg cell-mediated function, which can prevent Th1 cell-mediated inflammation and interferon-γ secretion (49), its lower levels found in patients with AITD with more severe disease could be associated with a defective Treg function previously reported in patients with AITD (50).

miRNA-21-5p, itself, was associated with a higher risk of developing GD and a worse clinical outcome, and it was correlated to persistent disease in the long-term follow-up, with a better predictive value than the currently used TRAb levels (51). Recent reports have highly implicated miR-21 in the regulation of immune functions and development of several autoimmune disorders (52–55), suggesting a shared mechanism of action of this miRNA in different immune cells. The fact that expression of miR-21 affects T-cell activation, including the Th1/Th2 balance and Th17 differentiation (20, 21, 36, 56, 57), may explain these findings. In fact, we have recently reported increased levels of pathogenic Th17 cells in the peripheral blood and thyroid tissue from patients with AITD (58, 59). Our results also point to a similar behavior between miR-21-5p and miR-96-5p in AITD serum samples. Recent findings have demonstrated that miR-96 is highly expressed in pathogenic Th17 cells, and its overexpression in CD4+ T cells significantly increases cytokine production of Th17 cells (37), denoting a role in Th17 cells (60).

For miR-142-3p and miR-301a-3p, there have been reports of their implication in Treg and Th17 regulation, respectively, in some autoimmune diseases (34, 35, 61, 62). However, to our knowledge, data are still lacking regarding these miRNAs in AITD, and our results add new evidence to their role in Treg dysregulation in this particular disease (50) (Fig. 3B).

In summary, our data reveal for the first time using NGS, to our knowledge, the validation of dysregulated miRNAs in thyroid tissue and serum from patients with AITD. In addition, we provide a five-signature miRNA, which may be used as a potential biomarker to assign a risk for developing AITD and also for the evaluation of the severity of GD. This signature could have a substantial value in selecting specific treatment options. These outcomes represent a meaningful advance in the field of miRNAs as biomarkers in AITD and could contribute to a better understanding of the powerful translational role of miRNAs.

Acknowledgments

We thank the Institut d'Investigació en Ciències de la Salut Germans Trias i Pujol (IGTP-HUGTIP) Biobank and the Department of Surgery of Hospital Universitario la Princesa (HUP) (José Luis Muñoz) for providing tissue samples. We also thank our colleagues from the Department of Pathological Anatomy of HUP, especially Magdalena Adrados, for her help classifying thyroid specimens.

Financial Support: This work was supported by grants from the Ministerio de Economia y Competitividad and from the Instituto de Salud Carlos III [Proyectos de Investigación en Salud (FIS): PI13-01414, PI16-02091, and PIE13-0004-BIOIMID project] to M.M., and by grants from CIBER de Enfermedades Cardiovasculares (CIBERCV) and SAF2017-82886-R to F.S.-M. and cofinanced by FEDER funds.

Correspondence and Reprint Requests: Mónica Marazuela, MD, PhD, Department of Endocrinology, Hospital Universitario de la Princesa, Instituto de Investigación Princesa, Universidad Autónoma de Madrid, C/ Diego de León 62, 28006 Madrid, Spain. E-mail: monica.marazuela@salud.madrid.org.

Disclosure Summary: The authors have nothing to disclose.

References

1. Ramos-Leví AM, Marazuela M. Pathogenesis of thyroid autoimmune disease: the role of cellular mechanisms. *Endocrinol Nutr*. 2016;**63**(8):421–429.
2. Weetman AP. Autoimmune thyroid disease. *Autoimmunity*. 2009;**37**(4):337–340.
3. Weetman AP. Cellular immune responses in autoimmune thyroid disease. *Clin Endocrinol (Oxf)*. 2004;**61**(4):405–413.
4. Bartalena L, Fatourechi V. Extrathyroidal manifestations of Graves' disease: a 2014 update. *J Endocrinol Invest*. 2014;**37**(8):691–700.
5. Bartel DP. MicroRNAs: genomics, biogenesis, mechanism, and function. *Cell*. 2004;**116**(2):281–297.
6. Kozomara A, Griffiths-Jones S. miRBase: annotating high confidence microRNAs using deep sequencing data. *Nucleic Acids Res*. 2013;**42**(D1):D68–D73.
7. Heegaard NHH, Carlsen AL, Skovgaard K, Heegaard PMH. Circulating extracellular microRNA in systemic autoimmunity. *EXS*. 2015;**106**:171–195.
8. Nakamachi Y, Kawano S, Takenokuchi M, Nishimura K, Sakai Y, Chin T, Saura R, Kurosaka M, Kumagai S. MicroRNA-124a is a key regulator of proliferation and monocyte chemoattractant protein 1 secretion in fibroblast-like synoviocytes from patients with rheumatoid arthritis. *Arthritis Rheum*. 2009;**60**(5):1294–1304.
9. Wang H, Peng W, Ouyang X, Li W, Dai Y. Circulating microRNAs as candidate biomarkers in patients with systemic lupus erythematosus. *Transl Res*. 2012;**160**(3):198–206.
10. Tang Y, Luo X, Cui H, Ni X, Yuan M, Guo Y, Huang X, Zhou H, de Vries N, Tak PP, Chen S, Shen N. MicroRNA-146A contributes to abnormal activation of the type I interferon pathway in human lupus by targeting the key signaling proteins. *Arthritis Rheum*. 2009;**60**(4):1065–1075.
11. Xia P, Fang X, Zhang ZH, Huang Q, Yan KX, Kang KF, Han L, Zheng ZZ. Dysregulation of miRNA146a versus IRAK1 induces

IL-17 persistence in the psoriatic skin lesions. *Immunol Lett*. 2012; **148**(2):151–162.
12. Bernecker C, Halim F, Lenz L, Haase M, Nguyen T, Ehlers M, Vordenbaeumen S, Schott M. microRNA expressions in CD4+ and CD8+ T-cell subsets in autoimmune thyroid diseases. *Exp Clin Endocrinol Diabetes*. 2014;**122**(2):107–112.
13. Bernecker C, Lenz L, Ostapczuk MS, Schinner S, Willenberg H, Ehlers M, Vordenbäumen S, Feldkamp J, Schott M. MicroRNAs miR-146a1, miR-155_2, and miR-200a1 are regulated in autoimmune thyroid diseases. *Thyroid*. 2012;**22**(12):1294–1295.
14. Dorris ER, Smyth P, O'Leary JJ, Sheils O. MIR141 expression differentiates hashimoto thyroiditis from PTC and benign thyrocytes in Irish archival thyroid tissues. *Front Endocrinol (Lausanne)*. 2012;**3**:102.
15. Kagawa T, Watanabe M, Inoue N, Otsu H, Saeki M, Katsumata Y, Takuse Y, Iwatani Y. Increases of microRNA let-7e in peripheral blood mononuclear cells in Hashimoto's disease. *Endocr J*. 2016; **63**(4):375–380.
16. Liu R, Ma X, Xu L, Wang D, Jiang X, Zhu W, Cui B, Ning G, Lin D, Wang S. Differential microRNA expression in peripheral blood mononuclear cells from Graves' disease patients. *J Clin Endocrinol Metab*. 2012;**97**(6):E968–E972.
17. Peng H, Liu Y, Tian J, Ma J, Tang X, Yang J, Rui K, Zhang Y, Mao C, Lu L, Xu H, Wang S. Decreased expression of microRNA-125a-3p upregulates interleukin-23 receptor in patients with Hashimoto's thyroiditis. *Immunol Res*. 2015;**62**(2):129–136.
18. Qin Q, Wang X, Yan N, Song RH, Cai TT, Zhang W, Guan LJ, Muhali FS, Zhang JA. Aberrant expression of miRNA and mRNAs in lesioned tissues of Graves' disease. *Cell Physiol Biochem*. 2015; **35**(5):1934–1942.
19. Shen L, Huang F, Ye L, Zhu W, Zhang X, Wang S, Wang W, Ning G. Circulating microRNA predicts insensitivity to glucocorticoid therapy in Graves' ophthalmopathy. *Endocrine*. 2015;**49**(2): 445–456.
20. Tong BD, Xiao MY, Zeng JX, Xiong W. miRNA-21 promotes fibrosis in orbital fibroblasts from thyroid-associated ophthalmopathy. *Mol Vis*. 2015;**21**:324–334.
21. Wang Z, Fan X, Zhang R, Lin Z, Lu T, Bai X, Li W, Zhao J, Zhang Q. Integrative analysis of mRNA and miRNA array data reveals the suppression of retinoic acid pathway in regulatory T cells of Graves' disease. *J Clin Endocrinol Metab*. 2014; **99**(12):E2620–E2627.
22. Wei H, Guan M, Qin Y, Xie C, Fu X, Gao F, Xue Y. Circulating levels of miR-146a and IL-17 are significantly correlated with the clinical activity of Graves' ophthalmopathy. *Endocr J*. 2014; **61**(11):1087–1092.
23. Yamada H, Itoh M, Hiratsuka I, Hashimoto S. Circulating microRNAs in autoimmune thyroid diseases. *Clin Endocrinol (Oxf)*. 2014;**81**(2):276–281.
24. Zhu J, Zhang Y, Zhang W, Zhang W, Fan L, Wang L, Liu Y, Liu S, Guo Y, Wang Y, Yi J, Yan Q, Wang Z, Huang G. MicroRNA-142-5p contributes to Hashimoto's thyroiditis by targeting CLDN1. *J Transl Med*. 2016;**14**(1):166.
25. Lee JY, Yun M, Paik JS, Lee SB, Yang SW. PDGF-BB enhances the proliferation of cells in human orbital fibroblasts by suppressing PDCD4 expression via up-regulation of microRNA-21. *Invest Ophthalmol Vis Sci*. 2016;**57**(3):908–913.
26. Hiratsuka I, Yamada H, Munetsuna E, Hashimoto S, Itoh M. Circulating microRNAs in Graves' disease in relation to clinical activity. *Thyroid*. 2016;**26**(10):1431–1440.
27. Pohl M, Grabellus F, Worm K, Arnold G, Walz M, Schmid KW, Sheu-Grabellus SY. Intermediate microRNA expression profile in Graves' disease falls between that of normal thyroid tissue and papillary thyroid carcinoma. *J Clin Pathol*. 2016;**70**(1):33–39.
28. Vandesompele J, De Preter K, Pattyn F, Poppe B, Van Roy N, De Paepe A, Speleman F. Accurate normalization of real-time quantitative RT-PCR data by geometric averaging of multiple internal control genes. *Genome Biol*. 2002;**3**:RESEARCH0034.
29. Andersen CL, Jensen JL, Ørntoft TF. Normalization of real-time quantitative reverse transcription-PCR data: a model-based variance estimation approach to identify genes suited for normalization, applied to bladder and colon cancer data sets. *Cancer Res*. 2004;**64**(15):5245–5250.
30. Marabita F, de Candia P, Torri A, Tegnér J, Abrignani S, Rossi RL. Normalization of circulating microRNA expression data obtained by quantitative real-time RT-PCR. *Brief Bioinform*. 2015;**17**(2): 204–212.
31. Ameling S, Kacprowski T, Chilukoti RK, Malsch C, Liebscher V, Suhre K, Pietzner M, Friedrich N, Homuth G, Hammer E, Völker U. Associations of circulating plasma microRNAs with age, body mass index and sex in a population-based study. *BMC Med Genomics*. 2015;**8**(1):61.
32. Okoye IS, Coomes SM, Pelly VS, Czieso S, Papayannopoulos V, Tolmachova T, Seabra MC, Wilson MS. MicroRNA-containing T-regulatory-cell-derived exosomes suppress pathogenic T helper 1 cells. *Immunity*. 2014;**41**(1):89–103.
33. O'Connell RM, Rao DS, Baltimore D. MicroRNA regulation of inflammatory responses. *Annu Rev Immunol*. 2012;**30**(1): 295–312.
34. Mycko MP, Cichalewska M, Machlanska A, Cwiklinska H, Mariasiewicz M, Selmaj KW. MicroRNA-301a regulation of a T-helper 17 immune response controls autoimmune demyelination. *Proc Natl Acad Sci USA*. 2012;**109**(20):E1248–E1257.
35. Huang B, Zhao J, Lei Z, Shen S, Li D, Shen GX, Zhang GM, Feng ZH. miR-142-3p restricts cAMP production in CD4+CD25- T cells and CD4+CD25+ TREG cells by targeting AC9 mRNA. *EMBO Rep*. 2008;**10**(2):180–185.
36. Garo LP, Murugaiyan G. Contribution of microRNAs to autoimmune diseases. *Cell Mol Life Sci*. 2016;**73**(10):2041–2051.
37. Ichiyama K, Gonzalez-Martin A, Kim BS, Jin HY, Jin W, Xu W, Sabouri-Ghomi M, Xu S, Zheng P, Xiao C, Dong C. The microRNA-183-96-182 cluster promotes T helper 17 cell pathogenicity by negatively regulating transcription factor Foxo1 expression. *Immunity*. 2016;**44**(6):1284–1298.
38. Wang J, Chen J, Sen S. MicroRNA as biomarkers and diagnostics. *J Cell Physiol*. 2015;**231**(1):25–30.
39. Abou-Zeid A, Saad M, Soliman E. MicroRNA 146a expression in rheumatoid arthritis: association with tumor necrosis factor-alpha and disease activity. *Genet Test Mol Biomarkers*. 2011;**15**(11): 807–812.
40. Kohlhaas S, Garden OA, Scudamore C, Turner M, Okkenhaug K, Vigorito E. Cutting edge: the Foxp3 target miR-155 contributes to the development of regulatory T cells. *J Immunol*. 2009;**182**(5): 2578–2582.
41. Lu LF, Boldin MP, Chaudhry A, Lin LL, Taganov KD, Hanada T, Yoshimura A, Baltimore D, Rudensky AY. Function of miR-146a in controlling Treg cell-mediated regulation of Th1 responses. *Cell*. 2010;**142**(6):914–929.
42. Yao R, Ma YL, Liang W, Li HH, Ma ZJ, Yu X, Liao YH. MicroRNA-155 modulates Treg and Th17 cells differentiation and Th17 cell function by targeting SOCS1. *PLoS One*. 2012;**7**(10): e46082.
43. Taganov KD, Boldin MP, Chang KJ, Baltimore D. NF-kappaB-dependent induction of microRNA miR-146, an inhibitor targeted to signaling proteins of innate immune responses. *Proc Natl Acad Sci USA*. 2006;**103**(33):12481–12486.
44. Rodríguez-Muñoz A, Martínez-Hernández R, Ramos-Leví AM, Serrano-Somavilla A, González-Amaro R, Sánchez-Madrid F, de la Fuente H, Marazuela M. Circulating microvesicles regulate Treg and Th17 differentiation in human autoimmune thyroid disorders. *J Clin Endocrinol Metab*. 2015;**100**(12):E1531–E1539.
45. Glud M, Klausen M, Gniadecki R, Rossing M, Hastrup N, Nielsen FC, Drzewiecki KT. MicroRNA expression in melanocytic nevi: the usefulness of formalin-fixed, paraffin-embedded material for miRNA microarray profiling. *J Invest Dermatol*. 2009;**129**(5): 1219–1224.

46. Klopfleisch R, Weiss AT, Gruber AD. Excavation of a buried treasure—DNA, mRNA, miRNA and protein analysis in formalin fixed, paraffin embedded tissues. *Histol Histopathol*. 2011;**26**(6):797–810.
47. Li J, Smyth P, Flavin R, Cahill S, Denning K, Aherne S, Guenther SM, O'Leary JJ, Sheils O. Comparison of miRNA expression patterns using total RNA extracted from matched samples of formalin-fixed paraffin-embedded (FFPE) cells and snap frozen cells. *BMC Biotechnol*. 2007;**7**(1):36.
48. Xi Y, Nakajima G, Gavin E, Morris CG, Kudo K, Hayashi K, Ju J. Systematic analysis of microRNA expression of RNA extracted from fresh frozen and formalin-fixed paraffin-embedded samples. *RNA*. 2007;**13**(10):1668–1674.
49. Gandhi R, Healy B, Gholipour T, Egorova S, Musallam A, Hussain MS, Nejad P, Patel B, Hei H, Khoury S, Quintana F, Kivisakk P, Chitnis T, Weiner HL. Circulating microRNAs as biomarkers for disease staging in multiple sclerosis. *Ann Neurol*. 2013;**73**(6):729–740.
50. Marazuela M, García-López MA, Figueroa-Vega N, de la Fuente H, Alvarado-Sánchez B, Monsiváis-Urenda A, Sánchez-Madrid F, González-Amaro R. Regulatory T cells in human autoimmune thyroid disease. *J Clin Endocrinol Metab*. 2006;**91**(9):3639–3646.
51. Weetman AP. Graves' disease. *N Engl J Med*. 2000;**343**(17):1236–1248.
52. Fenoglio C, Cantoni C, De Riz M, Ridolfi E, Cortini F, Serpente M, Villa C, Comi C, Monaco F, Mellesi L, Valzelli S, Bresolin N, Galimberti D, Scarpini E. Expression and genetic analysis of miRNAs involved in CD4+ cell activation in patients with multiple sclerosis. *Neurosci Lett*. 2011;**504**(1):9–12.
53. Garchow BG, Bartulos Encinas O, Leung YT, Tsao PY, Eisenberg RA, Caricchio R, Obad S, Petri A, Kauppinen S, Kiriakidou M. Silencing of microRNA-21 in vivo ameliorates autoimmune splenomegaly in lupus mice. *EMBO Mol Med*. 2011;**3**(10):605–615.
54. Ruan Q, Wang T, Kameswaran V, Wei Q, Johnson DS, Matschinsky F, Shi W, Chen YH. The microRNA-21-PDCD4 axis prevents type 1 diabetes by blocking pancreatic beta cell death. *Proc Natl Acad Sci USA*. 2011;**108**(29):12030–12035.
55. Punga AR, Andersson M, Alimohammadi M, Punga T. Disease specific signature of circulating miR-150-5p and miR-21-5p in myasthenia gravis patients. *J Neurol Sci*. 2015;**356**(1–2):90–96.
56. Murugaiyan G, da Cunha AP, Ajay AK, Joller N, Garo LP, Kumaradevan S, Yosef N, Vaidya VS, Weiner HL. MicroRNA-21 promotes Th17 differentiation and mediates experimental autoimmune encephalomyelitis. *J Clin Invest*. 2015;**125**(3):1069–1080.
57. Wang S, Wan X, Ruan Q. The microRNA-21 in autoimmune diseases. *Int J Mol Sci*. 2016;**17**(6):864.
58. Vitales-Noyola M, Ramos-Levi AM, Martínez-Hernández R, Serrano-Somavilla A, Sampedro-Nuñez M, González-Amaro R, Marazuela M. Pathogenic Th17 and Th22 cells are increased in patients with autoimmune thyroid disorders. *Endocrine*. 2017;**57**(3):409–417.
59. Figueroa-Vega N, Alfonso-Pérez M, Benedicto I, Sánchez-Madrid F, González-Amaro R, Marazuela M. Increased circulating pro-inflammatory cytokines and Th17 lymphocytes in Hashimoto's thyroiditis. *J Clin Endocrinol Metab*. 2010;**95**(2):953–962.
60. González-Amaro R, Marazuela M. T regulatory (Treg) and T helper 17 (Th17) lymphocytes in thyroid autoimmunity. *Endocrine*. 2015;**52**(1):30–38.
61. Mandolesi G, De Vito F, Musella A, Gentile A, Bullitta S, Fresegna D, Sepman H, Di Sanza C, Haji N, Mori F, Buttari F, Perlas E, Ciotti MT, Hornstein E, Bozzoni I, Presutti C, Centonze D. miR-142-3p is a key regulator of IL-1β-dependent synaptopathy in neuroinflammation. *J Neurosci*. 2016;**37**(3):546–561.
62. Tang X, Yin K, Zhu H, Tian J, Shen D, Yi L, Rui K, Ma J, Xu H, Wang S. Correlation between the expression of microRNA-301a-3p and the proportion of Th17 cells in patients with rheumatoid arthritis. *Inflammation*. 2016;**39**(2):759–767.

Deafness and loss of cochlear hair cells in the absence of thyroid hormone transporters Slc16a2 (Mct8) and Slc16a10 (Mct10)

David S. Sharlin,Lily Ng,François Verrey,Theo J. Visser, Ye Liu,Rafal T. Olszewski, Michael Hoa,Heike Heuer, and Douglas Forrest

Sci Rep. 2018; 8: 4403.

Abstract

Transmembrane proteins that mediate the cellular uptake or efflux of thyroid hormone potentially provide a key level of control over neurodevelopment. In humans, defects in one such protein, solute carrier SLC16A2 (MCT8) are associated with psychomotor retardation. Other proteins that transport the active form of thyroid hormone triiodothyronine (T3) or its precursor thyroxine (T4) have been identified in vitro but the wider significance of such transporters in vivo is unclear. The development of the auditory system requires thyroid hormone and the cochlea is a primary target tissue. We have proposed that the compartmental anatomy of the cochlea would necessitate transport mechanisms to convey blood-borne hormone to target tissues. We report hearing loss in mice with mutations in Slc16a2 and a related gene Slc16a10 (Mct10, Tat1). Deficiency of both transporters results in retarded development of the sensory epithelium similar to impairment caused by hypothyroidism, compounded with a progressive degeneration of cochlear hair cells and loss of endocochlear potential. Administration of T3 largely restores the development of the sensory epithelium and limited auditory function, indicating the T3-sensitivity of defects in the sensory epithelium. The results indicate a necessity for thyroid hormone transporters in cochlear development and function

Comment

The Allan-Hearndon-Dudley syndrome (characterised by gross hypotonia, severe mental impairment with little or no speech capability progressing to death before age 10) is now known to be associated with mutations in the monocarboxylate transporter 8(MCT8) which is one of the transporters involved in T4 transport into neural tissue. The authors of this experimental study have investigated the role of MCT8 and MCT10 in the developing ear in mice. Although thyroid dysfunction is known to affect auditory function there are no data from patients with AHD syndrome. In mice these workers found hearing loss in those animals with a mutation in either of the transporters and noted that administration of T3 could almost completely restored the development of the cochlear sensory epithelium with improvement in hearing.

Med Sci Monit. 2018; 24: 6438–6448.

Identification of Key Pathways and Genes in Anaplastic Thyroid Carcinoma via Integrated Bioinformatics Analysis

Shengqing Hu, Yunfei Liao, and Lulu Chen

Background To provide a better understanding of anaplastic thyroid carcinoma (ATC) at the molecular level, this study aimed to identify the genes and key pathways associated with ATC by using integrated bioinformatics analysis.

Based on the microarray data GSE9115, GSE65144, and GSE53072 derived from the Gene Expression Omnibus, the differentially expressed genes (DEGs) between ATC samples and normal controls were identified. With DEGs, we performed a series of functional enrichment analyses. Then, a protein–protein interaction (PPI) network was constructed and visualized, with which the hub gene nodes were screened out. Finally, modules analysis for the PPI network was performed to further investigate the potential relationships between DEGs and ATC.

A total of 537 common DEGs were screened out from all 3 datasets, among which 247 genes were upregulated and 275 genes were downregulated. GO analysis indicated that upregulated DEGs were mainly involved in cell division and mitotic nuclear division and the downregulated DEGs were significantly enriched in ventricular cardiac muscle cell action potential. KEGG pathway analysis showed that the upregulated DEGs were mainly enriched in cell cycle and ECM-receptor interaction and the downregulated DEGs were mainly enriched in thyroid hormone synthesis, insulin resistance, and pathways in cancer. The top 10 hub genes in the constructed PPI network were CDK1, CCNB1, TOP2A, AURKB, CCNA2, BUB1, AURKA, CDC20, MAD2L1, and BUB1B. The modules analysis showed that genes in the top 2 significant modules of PPI network were mainly associated with mitotic cell cycle and positive regulation of mitosis, respectively.

Conclusions

We identified a series of key genes along with the pathways that were most closely related with ATC initiation and progression. Our results provide a more detailed molecular mechanism for the development of ATC, shedding light on the potential biomarkers and therapeutic targets.

Comment

Anaplastic thyroid cancer (ATC) accounts for less than 1% of thyroid malignancies but is a devastating disease with very poor prognosis. This study has analysed differentially expressed genes from microarray data to improve the understanding of genes and key pathways associated with ATC. These analytical techniques have shed light on important genes and pathways which will hopefully allow development of therapeutic targets for this disease as well as improving our understanding of the pathogenesis.

Meta-analysis of microarray datasets identify several chromosome segregation related cancer/testis genes potentially contributing to anaplastic thyroid carcinoma

Mu Liu , Yu-lu Qiu, , Tong Jin , Yin Zhou , Zhi-yuan Mao and Yong-jie Zhang

PeerJ. 2018; 6: e5822.

ABSTRACT

Aim. Anaplastic thyroid carcinoma (ATC) is the most lethal thyroid malignancy. Identification of novel drug targets is urgently needed.

Materials & Methods. We re-analyzed several GEO datasets by systematic retrieval and data merging. Differentially expressed genes (DEGs) were filtered out. We also performed pathway enrichment analysis to interpret the data. We predicted key genes based on protein–protein interaction networks, weighted gene co-expression network analysis and genes' cancer/testis expression pattern. We also further characterized these genes using data from the Cancer Genome Atlas (TCGA) project and gene ontology annotation.

Results. Cell cycle-related pathways were significantly enriched in upregulated genes in ATC. We identified TRIP13, DLGAP5, HJURP, CDKN3, NEK2, KIF15, TTK, KIF2C, AURKA and TPX2 as cell cycle-related key genes with cancer/testis expression pattern. We further uncovered that most of these putative key genes were critical components during chromosome segregation.

Conclusion. We predicted several key genes harboring potential therapeutic value in ATC. Cell cycle-related processes, especially chromosome segregation, may be the key to tumorigenesis and treatment of ATC.

Comment

This study of genes in ATC has noted that the upregulated genes in this disease were related to cell cycle pathways many of the genes were involved in chromosome segregation. Hence the study sheds new light on pathogenesis and potential treatment of ATC.

Thyroglobulin level at week 16 of pregnancy is superior to urinary iodine concentration in revealing preconceptual and first trimester iodine supply

Monika Katko, Andrea Anett Gazso, Ildiko Hircsu, Harjit Pal Bhattoa, Zsuzsanna Molnar, Bela Kovacs, David Andrasi, [3]Janos Aranyosi, Rita Makai, Lajos Veress, Olga Torok, Miklos Bodor, Laszlo Samson, and Endre V. Nagy

Matern Child Nutr. 2018 Jan; 14(1): e12470.

Abstract

Pregnant women are prone to iodine deficiency due to the increased need for iodine during gestation. Progress has recently occurred in establishing serum thyroglobulin (Tg) as an iodine status biomarker, but there is no accepted reference range for iodine sufficiency during pregnancy. An observational study was conducted in 164 pregnant women. At week 16 of gestation urinary iodine concentration (UIC), serum Tg, and thyroid functions were measured, and information on the type of iodine supplementation and smoking were recorded. The parameters of those who started iodine supplementation (≥150 μg/day) at least 4 weeks before pregnancy (n = 27), who started at the detection of pregnancy (n = 51), and who had no iodine supplementation (n = 74) were compared. Sufficient iodine supply was found in the studied population based on median UIC (162 μg/L). Iodine supplementation ≥150 μg/day resulted in higher median UIC regardless of its duration (nonusers: 130 μg/L vs. prepregnancy iodine starters: 240 μg/L, and pregnancy iodine starters: 205 μg/L, p < .001, and p = .023, respectively). Median Tg value of pregnancy starters was identical to that of nonusers (14.5 vs. 14.6 μg/L), whereas prepregnancy starters had lower median Tg (9.1 μg/L, p = .018). Serum Tg concentration at week 16 of pregnancy showed negative relationship (p = .010) with duration of iodine supplementation and positive relationship (p = .008) with smoking, a known interfering factor of iodine metabolism, by multiple regression analysis. Serum Tg at week 16 of pregnancy may be a promising biomarker of preconceptual and first trimester maternal iodine status, the critical early phase of foetal brain development.

Comment

Adequate iodine nutrition especially at the time of conception and in the 1st trimester is known to be critical for optimal fetal brain development. Currently iodine status is assessed by measurement of urinary iodine concentration but this method has limitations. This paper reports that serum thyroglobulin determination at 16 weeks gestation may be a suitable biomarker of preconception iodine status as well as first trimester status.

Maternal Iodine Insufficiency and Excess Are Associated with Adverse Effects on Fetal Growth: A Prospective Cohort Study in Wuhan, China

Renjuan Chen Qian Li Wenli Cui Xiaoyi Wang Qin Gao Chunrong Zhong Guoqiang SunXinlin Chen Guoping Xiong et al *The Journal of Nutrition*, Volume 148, Issue 11, 1 November 2018, Pages 1814–1820,https://doi.org/10.1093/jn/nxy182

Maternal iodine status has been suggested to affect birth outcomes. Few studies have focused on its effects on fetal growth during pregnancy.

Objective
This study aimed to assess maternal iodine status during early pregnancy and further examine the relation between maternal iodine status and fetal growth.
Methods
A total of 2087 singleton-pregnant women participating in the Tongji Maternal and Child Health Cohort study were involved. Urinary iodine concentration (UIC) and creatinine concentration were measured in spot urine samples collected in early pregnancy (<20 wk of gestation). Fetal head circumference (HC), femur length (FL), and estimated fetal weight (EFW) were evaluated by ultrasonography in each trimester. A multiple linear regression model was used to examine the association of iodine status with fetal growth characteristics, and a mixed-effects model was used to assess longitudinal effect.
Results
The median UIC and iodine-to-creatinine (I/Cr) ratio were 178 μg/L and 234 μg/g, respectively. The prevalence of insufficient iodine status (I/Cr ratio <150 μg/g) was 19.8%(*n* = 414), of adequate iodine status (150–249 μg/g) was 34.8% (*n* = 726), of iodine status above the requirements (250–499 μg/g) was 32.1% (*n* = 669), and of excessive iodine status (≥500 μg/g) was 13.3% (*n* = 278). Maternal iodine insufficiency was inversely associated with fetal FL in the second and third trimesters. In stratified analysis, significant interactions were found between maternal iodine status and age as well as parity (all $P < 0.05$). The longitudinal analyses showed negative associations of maternal insufficient, more than adequate, or excessive iodine status with fetal growth during pregnancy (all $P < 0.05$).
Conclusions
In central China, maternal iodine insufficiency and excess coexisted during early pregnancy and they both adversely affected fetal growth. There is an urgent need for ongoing monitoring of iodine status among vulnerable pregnant women in order to optimize iodine nutrition during pregnancy.

Iodine deficiency in pregnancy is known to result in impaired neurodevelopment but effects on fetal growth are less well understood. This study examined fetal head circumference, fetal femur length and estimated fetal fetal weight in large numbers of women with insufficient iodine status, adequate iodine status iodine status above requirements and excessive iodine status and found that iodine insufficiency and excess were both associated with adverse fetal growth indicating the importance of adequate iodine nutrition during pregnancy.

Subclinical Changes in Maternal Thyroid Function Parameters in Pregnancy and Fetal Growth

Lauren E. Johns, Kelly K. Ferguson, David E. Cantonwine, Bhramar Mukherjee, John D. Meeker, and Thomas F. McElrath

J Clin Endocrinol Metab 103: 1349–1358, 2018

Context: Overt thyroid disease in pregnancy is a known risk factor for abnormal fetal growth and development. Data on the effects of milder forms of variation in maternal thyroid function on intrauterine growth are less well examined.
Objective: We explored these associations using repeated thyroid hormone and ultrasound measurements.
Design, Setting, and Participants: Data were obtained from 439 pregnant women without diagnosed thyroid disease who were participants in a case-control study of preterm birth nested within an ongoing prospective birth cohort in Boston, Massachusetts.
Main Outcome Measures: Ultrasound and delivery indices of fetal growth were standardized to those measured in a larger population.
Results: At median 10, 18, and 26 weeks of gestation, we observed significant inverse associations between free thyroxine (FT4) and birth weight z scores, with the strongest association detected at median 10 weeks, at which time a 10% increase in FT4 was associated with a 0.02 z score decrease (;8.5 g) in birth weight (b = 20.41 for ln-transformed FT4; 95% confidence interval, 20.64 to 20.18). FT4 was also inversely associated with repeated measurements of estimated fetal weight, head circumference, and abdominal circumference. We observed weaker inverse associations for total T4 and a positive relationship between total triiodothyronine and birth weight z scores. We did not observe any associations for thyroid-stimulating hormone.
Conclusion: In pregnant women without overt thyroid disease, subclinical changes in thyroid function parameters may influence fetal growth.

The current emphasis in studies in thyroid disease and pregnancy is not the effects of overt disease which are well known and accepted but the more subtle effects of maternal thyroid hormone concentrations within normal ranges with no thyroid disease.
This study reports the effects of thyroid hormone variation within the normal range and measures of fetal growth. This was particularly seen when examining the inverse relation between FT4 and birth weight. The underlying physiological reason for this observation is not clear but may be related to placental function implying appropriate nutrient transfer to the fetus as well as T4 transfer.

Immune-Related Thyroiditis with Immune Checkpoint Inhibitors

Priyanka C. Iyer,Maria E. Cabanillas,Steven G. Waguespack, Mimi I. Hu, Sonali Thosani, Victor R. Lavis, Naifa L. Busaidy,Sumit K. Subudhi,Adi Diab,and Ramona Dadu[1]

THYROID Volume 28, Number 10, 2018 1243-1251

Background: Although immune-related thyroiditis (irT) with immune checkpoint inhibitors (ICI) is a common consequence, its natural course and management recommendations are not well characterized in existing guidelines. This study sought to investigate the evolution of irT and describe its course and sequelae.
Methods: This was a retrospective study of cancer patients treated with ICI between November 2014 and July2016 at MD Anderson Cancer Center and referred for endocrinology evaluation for suspected irT. Patients included had normal baseline thyroid function tests prior to starting ICI and developed thyrotoxicosis due to irT.
Results: Of 657 patients treated with ICI during the study period, 43(6.5%) met the inclusion criteria. ICI included: ipilimumab + nivolumab (40%), nivolumab (33%), pembrolizumab (21%), and other (7%). Cancer diagnoses observed were melanoma (23%), renal-cell carcinoma (21%), lung cancer (19%), bladder cancer (12%),colon cancer (9%), and other cancers (15%). Median time from ICI start to thyrotoxicosis was 5.3 weeks (range0.6–19.6 weeks). Clinically, patients presented with painless thyroiditis, and 67% were asymptomatic during the thyrotoxicosis phase. Thyrotoxicosis lasted a median of six weeks (range 2.6–39.7 weeks). Hypothyroidism developed in 37 (84%) patients at a median of 10.4 weeks (range 3.4–48.7 weeks) after starting ICI. These patients remained on levothyroxine and ICI at a median follow-up of 57.4 weeks (range 1–156.7 weeks) from hypothyroidism onset. Four patients recovered without initiating levothyroxine and remained euthyroid at a median follow-up of 11.35 months (range 4.43–14.43 months). Subgroup analysis of ipilimumab + nivolumab versus nivolumab alone showed a median time to thyrotoxicosis of two weeks [confidence interval (CI) 3.5–8.4] versus six weeks ([CI 1.2–2.8]; p = 0.26) and time to hypothyroidism of 10 weeks [CI 8.1–11.9] versus 17 weeks ([CI8.8–25.2]; p = 0.029) after starting ICI. Thyroid peroxidase and thyroglobulin antibodies were present in 45% and33% at the time of irT diagnosis.
Conclusions: IrT manifests as an early onset of thyrotoxicosis, which is largely asymptomatic, followed by rapid transition to hypothyroidism requiring long-term levothyroxine substitution. The evolution of irT is more rapid with combination ICI. Frequent monitoring of thyroid function tests during ICI is warranted. Future guidelinesneed to recognize this entity and incorporate their management.

Comment

Immune checkpoint inhibitors have transformed the treatment of some cancers but they can have alarming side effects. This retrospective study found 6.5% of patients with thyroiditis characterised by a similar clinical pattern to post partum thyroiditis namely onset of thyrotoxicosis followed by hypothyroidism requiring long term thyroxine therapy. This clinical picture is more rapid in patients receiving combination therapy.

Performance of a Multigene Genomic Classifier in Thyroid Nodules With Indeterminate Cytology A Prospective Blinded Multicenter Study

David L. Steward, Sally E. Carty,; Rebecca S. Sippel, Samantha Peiling Yang, Julie A. Sosa, Jennifer A. Sipos, James J. Figge, Susan Mandel, MD, MPH;Raja R. Seethala, William E. Gooding, Simion I. Chiosea, Cristiane Gomes-Lima, Robert L. Ferris, Jessica M. Folek, Raheela A. Khawaja, Priya Kundra Kwok Seng Loh, Carrie B. Marshall, Sarah Mayson, Kelly L. McCoy, Min En Nga, Kee Yuan Ngiam, Marina N. Nikiforova, Jennifer L. Poehls, Matthew D. Ringel, MD;Huaitao Yang, Md, PhD; Linwah Yip, MD; Yuri E. Nikiforov, MD, PhD
JAMA Oncol. doi:10.1001/jamaoncol.2018.4616

IMPORTANCE Approximately 20%of fine-needle aspirations (FNA) of thyroid nodules have indeterminate cytology, most frequently Bethesda category III or IV. Diagnostic surgeries can be avoided for these patients if the nodules are reliably diagnosed as benign without surgery.
OBJECTIVE To determine the diagnostic accuracy of a multigene classifier (GC) test (ThyroSeq v3) for cytologically indeterminate thyroid nodules.
DESIGN, SETTING, AND PARTICIPANTS Prospective, blinded cohort study conducted at 10 medical centers, with 782 patients with 1013 nodules enrolled. Eligibility criteria were met in 256 patients with 286 nodules; central pathology review was performed on 274 nodules.
INTERVENTIONS A total of 286 FNA samples from thyroid nodules underwent molecular analysis using the multigene GC (ThyroSeq v3).
MAIN OUTCOMES AND MEASURES The primary outcome was diagnostic accuracy of the test for thyroid nodules with Bethesda III and IV cytology. The secondary outcome was prediction of cancer by specific genetic alterations in Bethesda III to V nodules.
RESULTS Of the 286 cytologically indeterminate nodules, 206 (72%) were benign, 69 (24%) malignant, and 11 (4%) non invasive follicular thyroid neoplasms with papillary-like nuclei (NIFTP). A total of 257 (90%) nodules (154 Bethesda III, 93 Bethesda IV, and 10 Bethesda V) had informative GC analysis, with 61%classified as negative and 39%as positive. In Bethesda III and IV nodules combined, the test demonstrated a 94%(95%CI, 86%-98%) sensitivity and 82%(95%CI, 75%-87%) specificity. With a cancer/NIFTP prevalence of 28%, the negative predictive value (NPV) was 97%(95%CI, 93%-99%) and the positive predictive value (PPV) was 66%(95%CI, 56%-75%). The observed 3%false-negative rate was similar to that of benign cytology, and the missed cancers were all low-risk tumors. Among nodules testing positive, specific groups of genetic alterations had cancer probabilities varying from 59%to 100%.
CONCLUSIONS AND RELEVANCE In this prospective, blinded, multicenter study, the multigene GC test demonstrated a high sensitivity/NPV and reasonably high specificity/PPV, which may obviate diagnostic surgery in up to 61% of patients with Bethesda III to IV indeterminate nodules, and up to 82%of all benign nodules with indeterminate cytology. Information on specific genetic alterations obtained from FNA may help inform individualized treatment of patients with a positive test result.

COMMENT

Thyroid nodules are common and raise the possibility of malignancy. Around 20% FNA samples have indeterminate cytology.In this study a large number of FNA samples were subjected to molecular analysis using a multigene classifier to determine the diagnostic accuracy of this technique. There was a 3% false negative rate (low risk tumours) and a negative predictive value of 97%. It is suggested that this technique will inform individual patients' treatment in those with a positive FNA result.

Predictive score for the development or progression of Graves' orbitopathy in patients with newly diagnosed Graves' hyperthyroidism

Wilmar Wiersinga, Miloš Žarković, Luigi Bartalena, Simone Donati, Petros Perros, Onyebuchi Okosieme, Daniel Morris, Nicole Fichter, Jurg Lareida, Georg von Arx, Chantal Daumerie, Maria-Christina Burlacu, George Kahaly, Susanne Pitz, Biljana Beleslin, Jasmina Ćirić, Goksun Ayvaz, Onur Konuk, Füsun Baloş Törüner, Mario Salvi, Danila Covelli, Nicola Curro, Laszlo Hegedüs and Thomas Brix on behalf of EUGOGO (European Group on Graves' Orbitopathy

European Journal of Endocrinology (2018) **178**, 635–643

Abstract

Objective: To construct a predictive score for the development or progression of Graves' orbitopathy (GO) in Graves' hyperthyroidism (GH).
Design: Prospective observational study in patients with newly diagnosed GH, treated with antithyroid drugs (ATD) for 18 months at ten participating centers from EUGOGO in 8 European countries.
Methods: 348 patients were included with untreated GH but without obvious GO. Mixed effects logistic regression was used to determine the best predictors. A predictive score (called PREDIGO) was constructed.
Results: GO occurred in 15% (mild in 13% and moderate to severe in 2%), predominantly at 6–12 months after start of ATD. Independent baseline determinants for the development of GO were clinical activity score (assigned 5 points if score > 0), TSH-binding inhibitory immunoglobulins (2 points if TBII 2–10 U/L, 5 points if TBII > 10 U/L), duration of hyperthyroid symptoms (1 point if 1–4 months, 3 points if >4 months) and smoking (2 points if current smoker). Based on the odds ratio of each of these four determinants, a quantitative predictive score (called PREDIGO) was constructed ranging from 0 to 15 with higher scores denoting higher risk; positive and negative predictive values were 0.28 (95% CI 0.20–0.37) and 0.91 (95% CI 0.87–0.94) respectively.
Conclusions: In patients without GO at diagnosis, 15% will develop GO (13% mild, 2% moderate to severe) during subsequent treatment with ATD for 18 months. A predictive score called PREDIGO composed of four baseline determinants was better in predicting those patients who will not develop obvious GO than who will.

Comment

Graves orbitopathy (GO) affects patients independent of their thyroid status although it is more commonly seen in those with thyrotoxic Graves disease. Most of GO is mild or moderate in clinical severity but a significant minority develop severe, sometimes sight threatening disease. Graves hyperthyroid patients at presentation often do not have any symptoms or signs of GO thus raising the question of prediction of onset in this group. This study developed a predictive score (PREDIGO) designed to establish which patients would develop GO. In fact results indicated that the metric was better in predicting those patients who did not develop GO than those who did so. Nevertheless this metric will have valuable clinical importance.

Metal Coordinated Poly-Zinc-Liothyronine Provides Stable Circulating Triiodothyronine Levels in Hypothyroid Rats

THYROID Volume 28, Number 11, 2018 1425-1433

Rodrigo R. Da Conceic¸, Gustavo W. Fernandes, Tatiana L. Fonseca, Barbara M.L.C. Bocco,[2]and Antonio C. Bianco

Background: Liothyronine (LT3) has limited short-term clinical applications, all of which aim at suppressing thyrotropin (TSH) secretion. A more controversial application is chronic administration along with levothyroxine in the treatment of hypothyroidism. Long-term treatment with LT3 is complicated by its unique pharmacokinetics that result in a substantial triiodothyronine (T3) peak in the blood three to four hours after oral dosing. This is a
significant problem, given that T3 levels in the blood are normally stable, varying by <10% throughout the day.
Methods: A metal coordinated form of LT3 (Zn[T3][H2O])n, known as poly-zinc-liothyronine (PZL), was synthesized and loaded into coated gelatin capsules for delivery to the duodenum where sustained release of T3from PZL occurs. Male Wistar rats were made hypothyroid by feeding on a low iodine diet and water containing0.05% methimazole for five to six weeks. Rats were given a capsule containing 24 lg/kg PZL or equimolar amounts of LT3. Blood samples were obtained multiple times from the tail vein during the first 16 hours, and processed for T3 and TSH serum levels. Some animals were treated daily for eight days, and blood samples were
collected daily.
Results: Rats given LT3 exhibited the expected serum T3 peak (about fivefold baseline) at 3.5 hours, followed by a rapid decline, with serum levels almost returning to baseline values by 16 hours. In contrast, serum T3 in PZL treated rats exhibited about a 30% lower T3 peak at nine hours. Furthermore, the plateau time, that is, the time span during which the serum T3 concentration is at least half of T3 peak, increased from 4.9 to 7.7 hours in LT3-versus PZL-treated rats, respectively. Serum TSH dropped in both groups, but PZL-treated rats exhibited a more gradual decrease, which was delayed by about four hours compared to LT3-treated rats. Chronic treatment with either LT3 or PZL restored growth, lowered serum cholesterol, and stimulated hepatic expression of the Dio1mRNA and other T3-dependent markers in the central nervous system.
Conclusion: Capsules of PZL given orally restore T3-dependent biological effects while exhibiting a reduced and delayed serum T3 peak.

Comment

There is considerable controversy in the practice of thyroidology concerning the administration of T3 to patients who are receiving treatment with T4 for therapy of any form of hypothyroidism. In contrast to T4 the half life of available T3 preparations is short resulting in undesirable peaks of serum T3 sometimes associated with cardiac arrythmias. This paper reports the introduction of a long acting T3 and describes the pharmacokinetics in rats. The results suggest that this formulation should be evaluated in the human situation.